FAILURE ANALYSIS OF THICK COMPOSITES

A THESIS SUBMITTED TO
THE GRADUATE SCHOOL OF NATURAL AND APPLIED SCIENCES
OF
MIDDLE EAST TECHNICAL UNIVERSITY

BY

MELEK ESRA ERDEM

IN PARTIAL FULFILLMENT OF THE REQUIREMENTS
FOR
THE DEGREE OF MASTER OF SCIENCE
IN
MECHANICAL ENGINEERING

FEBRUARY 2013

Approval of the thesis:

FAILURE ANALYSIS OF THICK COMPOSITES

submitted by **MELEK ESRA ERDEM** in partial fulfillment of the requirements for the degree of **Master of Science in Mechanical Engineering Department, Middle East Technical University** by,

Prof. Dr. Canan Özgen   _____
Dean, Graduate School of **Natural and Applied Sciences**

Prof. Dr. Süha Oral   _____
Head of Department, **Mechanical Engineering**

Prof. Dr. K. Levend Parnas   _____
Supervisor, **Mechanical Engineering Dept., METU**

Examining Committee Members:

Prof. Dr. Haluk Darendeliler   _____
Mechanical Engineering Dept., METU

Prof. Dr. K. Levend Parnas   _____
Mechanical Engineering Dept., METU

Prof. Dr. Suat Kadıoğlu   _____
Mechanical Engineering Dept., METU

Asst. Prof. Dr. Ergin TÖNÜK   _____
Mechanical Engineering Dept., METU

Gökhan Tursun, M.Sc.   _____
Composite Structures Dept. Chief, TAI

Date: 01.02.2013

I hereby declare that all information in this document has been obtained and presented in accordance with academic rules and ethical conduct. I also declare that, as required by these rules and conduct, I have fully cited and referenced all material and results that are not original to this work.

Name, Last name: Melek Esra Erdem

Signature:

ABSTRACT

FAILURE ANALYSIS OF THICK COMPOSITES

Erdem, Melek Esra

M.Sc., Department of Mechanical Engineering

Supervisor: Prof. Dr. K. Levend Parnas

February 2013, 78 pages

A three-dimensional finite element model is constructed to predict the failure of a hybrid and thick laminate containing bolted joints. The results of the simulation are compared with test results. The simulation comprises two main challenging steps. Firstly, for a realistic model, a 3D model is established with geometric nonlinearities and contact is taken into account. The laminated composite model is constructed by 3D layered elements. The effect of different number of elements through the thickness is investigated. The failure prediction is the second part of the simulation study. Solutions with and without progressive failure approach are obtained and the effect of progressive failure analysis for an optimum simulation of failure is discussed. The most appropriate failure criteria to predict the failure of a thick composite structure is also investigated by considering various failure criteria. By comparing the test results with the ones found from the finite element analyses, the validity of the developed model and the chosen failure criteria are discussed.

Keywords: Thick Composites, Bolt Connection, Finite Element Analysis, Progressive Failure Method, Failure Criteria

ÖZ

KALIN KOMPOZİTLERİN HASAR ANALİZİ

Erdem, Melek Esra

Yüksek Lisans, Makina Mühendisliği Bölümü

Tez Yöneticisi: Prof. Dr. K. Levend Parnas

Şubat 2013, 78 sayfa

Hibrit, kalın kesitli ve cıvata bağlantısı olan tabakalı bir yapının hasar tahmini için üç boyutlu sonlu elemanlar modeli oluşturulmuştur. Simülasyon sonuçları test sonuçlarıyla karşılaştırılmıştır. Simülasyon aşaması iki adımdan oluşmaktadır. Öncelikle, gerçekçi bir modelleme için 3 boyutlu bir model, lineer olmayan geometri ve temas göz önünde bulundurularak oluşturulmuştur. Kompozit tabakalı yapı modeli 3 boyutlu tabakalı elemanlarla yapılmıştır. Kalınlık boyunca farklı sayıda eleman kullanmanın etkisi incelenmiştir. Hasarın tahmini simülasyon çalışmasının ikinci kısmıdır. İlerleyen hasar yöntemiyle ve bu yöntem kullanılmadan hesaplamalar yapılmış ve hasarın optimum simülasyonu için ilerleyen hasar yönteminin etkisi tartışılmıştır. Kalın kompozit yapının hasar tahmininde kullanılması için en uygun hasar kriteri, çeşitli kriterler değerlendirilerek belirlenmiştir. Testlerin ve sonlu eleman analizlerinin sonuçları karşılaştırılarak, modelin ve seçilen hasar kriterinin geçerliliği tartışılmıştır.

Anahtar Kelimeler: Kalın Kompozitler, Cıvatalı Bağlantı, Sonlu Elemanlar Yöntemi, İlerleyen Hasar Yöntemi, Hasar Kriteri

ACKNOWLEDGEMENTS

TABLE OF CONTENTS

LIST OF TABLES

LIST OF FIGURES

FIGURES

LIST OF SYMBOLS AND ABBREVATIONS

Symbols

σ_{ij}	Stress tensor
ε_{ij}	Strain tensor
C_{ij}	Stiffness matrix
E_i	Young's moduli in ith direction
G_{ij}	Shear modulus
ν_{ij}	Poisson's ratio
X_t, X_c	axial or longitudinal strength under tension, compression
Y_t, Y_c	transverse strength in 2-direction under tension, compression
Z_t, Z_c	transverse strength in 3-direction under tension, compression
S_{ij}	shear strength in i,j=1,2,3, i≠j
e_{1t}, e_{1c}	maximum allowable strain in 1 direction under tension, compression
e_{2t}, e_{2c}	maximum allowable strain in 2 direction under tension, compression
e_{3t}, e_{3c}	maximum allowable strain in 3 direction under tension, compression
g_{ij}	maximum allowable shear strain in i,j=1,2,3, i≠j
ρ	density, [kg/mm^3]
D	diameter [mm]
Ø	diameter [mm]
K	Ramberg-Osgood coefficient [MPa]
n	Ramberg-Osgood exponent
t	time [s]

Abbreviations

CLT	Classical lamination theory
FEA	Finite element analysis
FEM	Finite element method
FI	Failure Index
FPF	First Ply Failure
FRP	Fiber reinforced plastic
FSDT	First order shear deformation theory
LVDT	Linear variable differential transducer
PFA	Progressive failure analysis
UD	Unidirectional
WWFE	World-Wide Failure Exercise

Common Indices

P_t	Property under tension loading
P_c	Property under compression loading

CHAPTER 1

INTRODUCTION

Composite materials are formed by combining two or more materials on macroscopic scale in order to obtain improved properties over the constituent materials. It has been more than half a century since polymeric-based composite materials were offered and composites become a frequently used material of many industrial applications in a short time [1].

The reason for composites to spread very fast is the various advantages they offer. High strength-to-weight and stiffness-to-weight ratios, favorable corrosion resistance and fatigue life characteristics, enabling manufacturing of complex geometries easier are the most important factors making composites preferable. Since they present high performance in lower weight compared to metallic parts, 20 to 80% of weight gain can be obtained by substituting metal parts with composites[1].

In the past, application of composite materials was limited to structurally not very critical, thin cross-sectioned, geometrically simple members; and a vast amount of knowledge on these structures has been generated in literature. With the experience gathered on composites, the courage came out to use these materials in primary structures, especially to take the advantage of weight gain. However, applying the design, analysis and test methods developed for thin-sectioned composite structures directly to thick-sectioned could not give satisfactorily accurate results [2], and researches to construct reliable and standardized methods for thick-sectioned as well were started then. Although composite structures are being used as thick-sectioned widely now, there is still a considerable amount of unknown in mechanical properties to numerical modeling, failure criteria to be used to test methods of thick-sectioned composite structures. Thus, these are all very critical and active topics of research at present.

Failure of thick composite structures is a very significant subject among these active research topics. The use of composite materials is very advantageous in many applications; however, designing and analyzing these structures is not so easy because response of the composite structure to loading is dependent on the fiber orientation and stacking sequence because they are heterogeneous and anisotropic. Furthermore, both in plane and out-of-plane failures occur at the same time. These make it complicated to predict the failure mechanism. With the failure mechanism, initiation of damage, growth of it and final structural collapse is implied. On the other hand, if composite is used in structural members, like in the case of most thick structures exploring failure mechanism is crucial. Only ply–based failure criteria are not sufficient to monitor these mechanisms and they should be combined with appropriate damage models [3]. Both finding the right failure mechanism and choosing the appropriate failure criteria are serious problems to be dealt with.

Another important research topic is design of connection regions. Structure is weak in the vicinity of connections, and joint efficiencies of composite structures are even lower than metals. Thus, sometimes these critical areas are designed over-safe, using more than enough material in order to guarantee that the connections can withstand operation loads. However, in order to fully benefit from the weight advantage over metallic materials, the part shall be designed with just enough amount of material while carrying the loads exerted safely. Another approach for joint design is referring to test results, which is an expensive

method to choose. Hence, reliable analysis methods are needed to support the optimum design of joint areas and to reduce the number of tests required [4].

From the design point of view, the integrity of the structure under operation loads shall be proved, the maximum load that the structure can withstand and the mode of failure shall be known. In this study, a reliable method to introduce the aforementioned information is aimed to found for thick composite structures. The best method to model thick composite structure with a bolt-connection is investigated. For a good simulation of failure, progressive failure analysis method is followed and the most appropriate failure criteria to be used are searched for. Afterwards, static tests are performed. The compatibility of the model and the chosen failure criteria is discussed by comparing the results from the tests with the results obtained from the finite element analysis.

1.1. Scope of Thesis

Finite element analysis and testing of a thick composite structure are conducted in the scope of this thesis. The thick structure with bolt-connection is constructed by stacking-up of carbon fabric plies, glass UD plies and foam material.

A 3D model is established for the finite element analysis of the thick structure. 3D modeling issues and the effect of modeling with different number of elements through the thickness are investigated.

For failure prediction, analyses both with and without progressive failure approach are executed. The influence of utilizing different failure criteria is discussed.

The effect of material properties and the material models to simulation are also debated.

For the verification of the finite element analysis only tension test is conducted.

The aim of this study is to find the most suitable numerical approaches to model thick composite structures and to specify the right failure model and failure criteria combinations to accurately predict failure. The more accurate analysis methods is accomplished, the more weight reduction, the less test needs, and the more time and money saving is possible.

1.2. Outline of Thesis

Outline of the thesis is as follows: This chapter introduces the scope and outline of the thesis. Chapter 2 gives a brief description for the composite materials, problems encountered in modeling of thick composite structures, problems of material property determination, progressive failure analysis method and failure criteria. In Chapter 3, a very brief theoretical background of the composite materials and the failure criteria are depicted. In Chapter 4, the analyzed structure in the scope of this thesis is described. The details of the numerical and experimental procedures followed are set forth. In Chapter 5, the results of the numerical analysis and tests are presented. A brief comparison of the results is also given. Finally, Chapter 6 presents the conclusions of this study. Comments are given for the possible causes of errors.

CHAPTER 2

LITERATURE SURVEY

2.1. Composite Materials

Composite materials are made by combining two or more materials to generate a material form exhibiting the desirable features that even the constituent materials does not possess alone. A development in the property of concern such as stiffness, strength, weight, corrosion resistance, fatigue life, acoustic insulation, thermal conductivity etc. is aimed. The constituents are combined on macroscopic scale and thus a nonhomogeneous product is established in which the constituents can be recognized even by naked eye [5].

Composite materials are constituted by reinforcing a matrix material by fibers (in long continuous or woven form), whiskers (short fibers) or particulates. A fiber reinforced composite material is a matrix material reinforced by strong, stiff fibers, i.e. carbon fiber reinforced epoxy resin [6]. In this construction, fibers are the main load carrying elements, and the matrix material is responsible for bonding fibers and creates a medium both enables load-transfer among fibers and protection against environmental conditions [7] .

The main property that the composite materials differ from metals is the directional dependence in stiffness and strength. This attribute is usually turned into an advantage by structural tailoring to maximize the desired property in the required direction for improved performance. This is achieved by constructing a laminate by stacking-up lamina [7, 8].

Composite materials can be served in the form named as prepreg (or preimpregnated) implying a semi-product that the fibers and the matrix are combined by special processes by prepreg manufacturers. Prepregs are usually preferred in the industry to achieve a better quality product.

2.2. Analysis of Thick Composite Structures

As mentioned in previous chapter, researches on composite structures have been predominantly concentrated on thin cross-sectioned parts. Nevertheless, thick composites have an extensive application area now and various approaches on these structures shall be developed likewise.

2.2.1. Problem of Finding Out-of Plane Material Properties

Accuracy of material properties is critical for analysis purposes in order to achieve successful approximations. Out-of-plane stresses induced on thick cross-sectioned structures due to multidirectional loads are not negligible, thus 3D material properties are needed for their analysis [4]. However, for a majority of materials only in-plane properties can be accessed via their manufacturer's specifications. Actually, there are not any standardized methods for determination of both in plane and out-of-plane properties of thick composites suggested yet.

To obtain out-of-plane properties, the mainstream technique followed by most existing analysis studies is to make some assumptions and estimate 3D properties by a modification

of 2D properties that are generally available. One of the assumptions is to apply correction factors to 2D properties. Although these correction factors are found by testing and take into account effects of property degradation can be induced by porosity, fiber waviness, etc. and stresses generated as a result of manufacturing processes, Czischon et al. still defend more trustworthy knowledge shall be available for such an important parameter of analyses [9]. What is more, the inconvenience of such a conversion is shown by an experimental study of Zimmermann et al. [2]. Another popular assumption for the 2D property modification is to assume properties in z and y directions are exactly the same. However, this approach can only be valid for the very special case that the laminate having only UD fibers laid-up only in one direction. Shepheard et al. points out even for this very restricted case, there is still no guarantee that the properties will be the same, since there can be always errors in manufacturing process [10].

In 2011 a report published by National Physics Laboratory [11] pointing out most of researches on material properties of thick composites merely focused on determination of out-of-plane material properties; however, determination of in-plane properties for these structures is also an equally difficult important problem. Standardized test procedures are only valid for thin composites and the writers are after the compatibility of these procedures for thick structures to find material properties under tension and compression loads. The approach is to first to choose a standard test of thin composites and then testing both standard and a thicker-larger coupon according to it. Consequently, it is concluded that if lamination of thick coupon is done following the loop of stacking sequence of the thin coupon, then in-plane properties are well matched. However, if the plies are grouped to resemble the same stacking sequence of thin coupon, then there is a fall off observed in strengths of thick coupon. Actually, the reduction in compression and tension strengths as a result of ply blocking was reached and introduced by many previous studies, i.e. [12, 13]. The more layers are grouped, the lower the strains matrix cracks at.

Compression tests and four point bending test for determination of out-of-plane properties with thick cross-sectioned specimens were performed by Shepheard et al. [10, 14] and Czichon et al. [9] proposed a modified three point bending method for thick composite structures. From compression tests, the comparison of properties of their thick coupon with standardized thin coupon, a decay of the properties for thicker coupon can be observed; which is claimed to be a result of quality variations of coupons by the authors. For four-point-bending test, they compared results with finite element analysis results and since a large difference exists, they proposed some correction factors.

2.2.2. Mechanical Joint Analysis

Joining of different parts is almost always required in a typical product construction for the transfer of the loads or to enable relative movement of parts with respect to each other. Parts can either be bonded by adhesives or mechanically joined. As a rule of thumb of design, joints shall be avoided as much as possible since they generate weak areas within the structure where the failure will possibly be originated from [1]. For instance, if there is a mechanical joint in a composite structure, there is local contact between the hole and the fastener, which may cause high stress concentrations, large strains and delamination mode of failure. These effects can even result in the ultimate failure of the structure. Thus, connection region design and analysis is a critical and an important topic for composites [15].

Most of the work until 21st century [16-19] considered the joint problem as 2D and utilized first order theories i.e. classical lamination theory and first order shear deformation theory (FSDT) for solutions. However, for joint problem neither 2D modeling nor the first order theories neglecting through-thickness effects are appropriate [4, 15]. The necessity of a 3D model for a reliable investigation of the joint problem stems from the 3D the stress state at the free edges i.e. holes. Due to the different orientations of the adjacent plies of laminate,

the Poisson's ratios differ from one ply to another which results in high interlaminar shear and normal stresses at the free edges and consequently a 3D stress-state [20].

Between the years 2000-2003 a project, BOJCAS (Bolted Joints in Composites Aircraft Structures), was conducted as a part of 5th Framework Programme of European Union to investigate safety and efficiency of the bolted joints in composite structures. Outputs of the project would be design and analysis methodologies and related software; these would be served to the use of aircraft industry of Europe [21]. Consequently, test needs for the joint validation would be decreased.

Within the scope of BOJCAS, both static and fatigue analyses of the joints were performed. For global models, models of usually large areas containing multi-bolt connections, two-dimensional finite element method was used in order to analyze faster. For analysis in local areas or analysis of the critical connection areas, three-dimensional progressive failure finite element analysis method was conducted. To combine the global and local analyses, a method was developed as well. All the methods generated were verified by tests [21]. What is missing in this comprehensive study is the structure was examined only under tension loads; neither bending nor combined load cases were investigated.

Another work on joint problem analyzed a thick laminate and evaluated delamination bearing strength [15]. Using layerwise theory and quasi-three-dimensional mesh, which is established by combining 8-node 2D elements with 3-node 1D element, stress distribution for every layer in transverse direction is calculated. Three dimensional contact stresses is taken into consideration. Failure is checked by modified Ye-delamination criterion. The tests performed to validate the model shows that the bearing stresses are underestimated by the model [22].

For final collapse of a laminate having a mechanical joint and in tension, the expected failures can be classified as;

- Net-tension (or Brittle)

- Shear-out (or pull-out)

- Delamination.

The diameter of the hole, laminate thickness and stacking sequence are the main parameters influences these failure behavior [23].
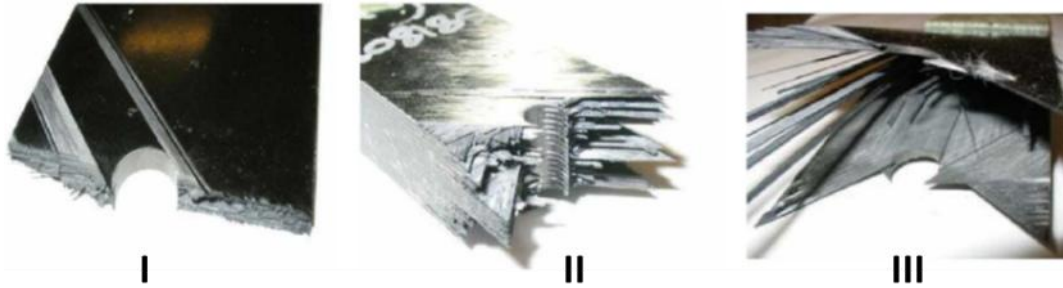
Figure 2.1 Failure types: (I) Net-tension, (II) Shear-out, (III) Delamination [23].

2.3. Failure Modeling

Most of the failure models make the assumption of the ultimate strengths of a lamina embedded in a laminate is very close to ultimate strength of the isolated lamina [24].

Failure analysis of a composite structure starts with the estimation of strains and stresses. Strains and stresses of single plies can be estimated employing Classical Lamination Theory (CLT). However, for FRP laminates, the non-linearity of the constitutive equations is significant and shall be regarded especially for in-plane shear and transverse compression cases; while it can be ignored in fiber direction [24, 25]. Another method for stress-strain calculation was utilized in the model of Bogetti et al. [26]. They employed three-dimensional laminated media analysis developed by Chou et al. [27]. Regarding the stresses and strains in thickness direction is the main difference of this method from the Classical Lamination Theory. What is more, in three-dimensional laminated media analysis the laminate is not allowed to deform to a curved shape, which well simulates the case for thick-sectioned composites structures. Nevertheless, results obtained by this method is very similar to ones obtained with CLT for in-plane laminate behavior and ply stress and strains if the laminate investigated is balanced and symmetric.

In real world, application of a loading alone or combined changes the shape of stress-strain diagrams. For simplicity the consequence of these interactions are usually neglected in analyses, i.e. the application of σ_1 alone or combined with another loading simultaneously does not cause any difference in stress-strain equations in fiber direction [25].

2.3.1. Progressive Failure Analysis

Progressive failure approach enables monitoring damage in the structure at all steps from initiation and propagation of failure to complete collapse.

The significance of progressive failure analysis for composite structures is an outcome of failure characteristics of composites; these materials actually fail in a progressive way. Failure starts with formation of one crack and with the increasing load more cracks emerged. However, these cracks do not prevent composite structure to carry the operation loads immediately after they are formed. For instance, if a fiber failed, the loading on it is transferred to intact fibers. Similarly, the structure cannot be assumed as completely failed after the damage of a single lamina, the load on it can be carried by intact lamina. Nonetheless, ultimate failure of the structure will be a consequence of these cracks; hence their formation and propagation will be followed. All these instances can be simulated by progressive failure analysis. The method also enables determining a more realistic result for

the loading that the composite cannot withstand any more. It facilitates optimization of design.

Performing a progressive failure analysis is possible utilizing many commercial finite element analysis tools. There are also various methods presented for the progressive failure modeling. Among these methods there are differences in the calculation of stresses and strains, in modes the failure checked and in the degradation methods. But the main logic of the method is first to calculate stresses and strains of the structure and put these in the relations of the selected failure criteria. If failure is obtained, then the stiffness of the failed elements is degraded and the load is redistributed. The stresses and strains are estimated with the reduced properties afterwards and the cycle starts again. If failure is not obtained, then load is increased. The process continues until ultimate failure load is reached. The structure is said to reach ultimate load if the stiffness of the structure is reduced such that excessive deformations and strains are obtained in the laminate, i.e. strain is larger than 5%. An example flow chart of the procedure is depicted in Figure 2.2.

The progressive failure analysis initiates with the estimation of strains and stresses. The assumption on the linearity of the material property affects the results of this preliminary step directly. Puck and Schürmann took into account the nonlinearity of material and estimated the stress-strain curves by third-order spline functions [25]. In the model of Bogetti et al. the nonlinear material response of the laminate is obtained by superimposing piece-wise linear stress-strain relations at each increment. Firstly, Ramberg-Osgood equation is applied on ply level to impose nonlinearity of material. Then, the stresses and strains are evaluated. The piece-wise linear increments make up the total effective nonlinear response. At each step, effective laminate stiffness matrix is updated depending on the instantaneous strain [26, 28].

Another important part of a progressive failure analysis is material degradation. The degraded properties shall not be recovered in the later increments of the analysis. There are various methods for degradation.

There are many studies in literature on progressive failure analysis. One of the important studies is presented in scope of aforementioned project BOJCAS [4]. To analyze three-bolted composite joints, they take the advantage of using a progressive damage finite element model; and thus eliminated the inconveniencies of former semi-empirical studies. Former studies examining multi-bolt composite joints needed a characteristic distance, which is found experimentally for every configuration of the structure, to investigate the failure for all modes of the bolt chosen as critical from an initial load distribution analysis. Furthermore, load re-distribution after the failure of the critical bolt was not calculated in these methods.
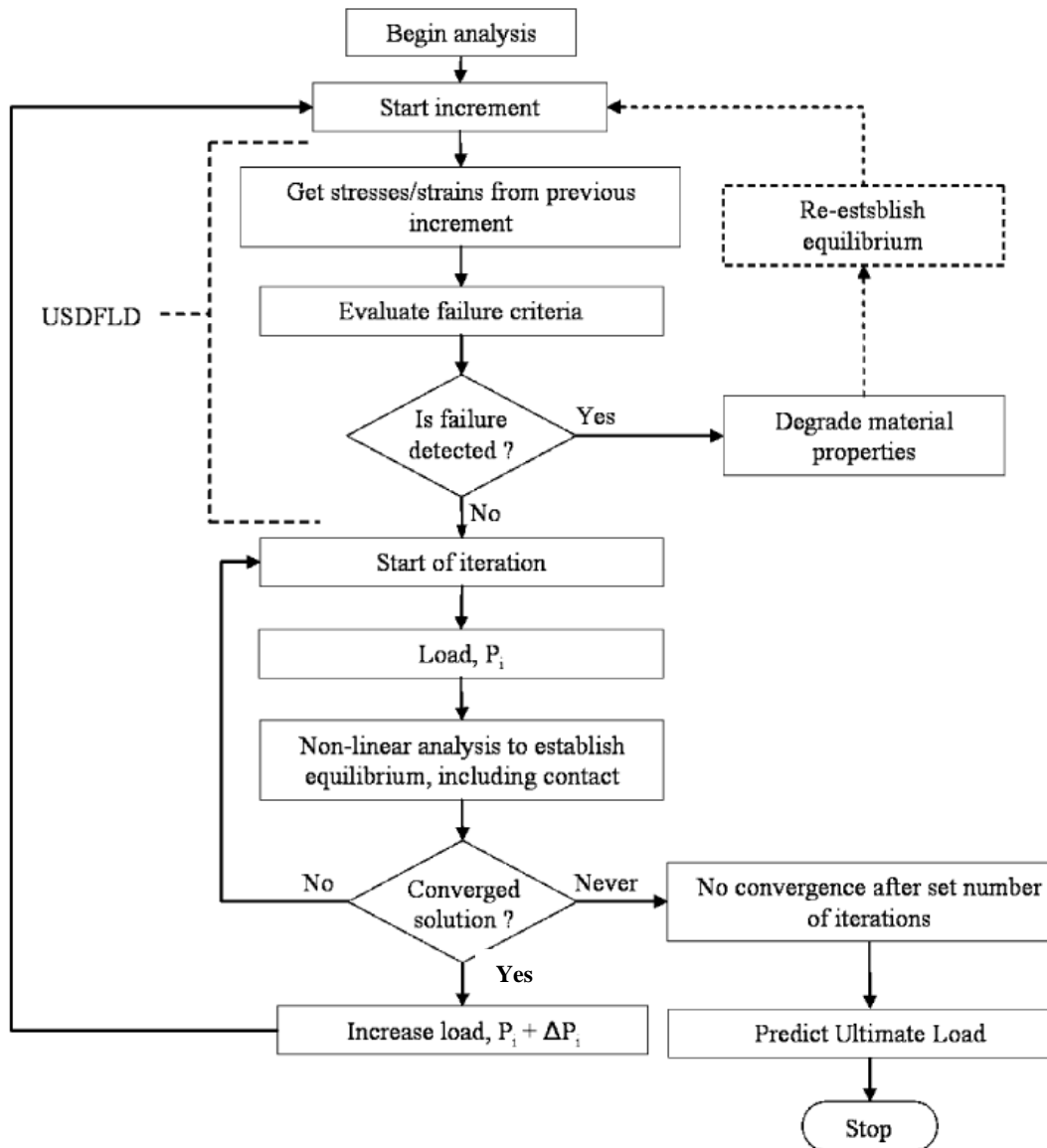
Figure 2.2 Example program flow chart for progressive failure analysis [4].

They constructed a three-dimensional model considering the contact phenomenon in commercial code ABAQUS and utilized the subroutine USDFLD to do a progressive failure analysis. Failure is checked by the program with Hashin failure criteria using stresses from the previous load increment. If failure is observed, the related stiffnesses with the failure mode are reduced to 10% of original value. After stiffness reduction, some studies assess the same load to see whether additional failures will take place or not; some argue that the change in stresses are negligible so that this check is not necessary. In this study, the load steps was very small, thus calculation of the same load is skipped.

Pineda et al. [29] worked on progressive damage of laminated fiber reinforced composites. To check failure two finite element models, global and micromechanics, are suggested.

Global model checks failure with 2D Hashin-Rotem failure criterion and micromechanics model utilizes 3D Tsai-Hill failure criterion for matrix and maximum stress criterion for fiber failure.

Cuntze [30] employs a non-linear three-dimensional progressive failure approach. For calculation of stresses for the non-linear analysis, stress-strain curves of both material hardening and material softening are utilized. In the load controlled hardening process the maximum strength is obtained which is also the failure onset stress of the inter fiber failure (IFF). After this point is reached, softening activates and the process turns into strain controlled and progressive failure analysis should start. The analysis is performed layer-by-layer. For degradation, rather than a ply discount method, a gradual reduction in the stiffness is preferred. This is both more realistic and causes fewer convergence problems. Though, there are approaches preferring an instantaneous decrease in properties and accomplished successful predictions [23, 31].

Puck and Schürmann have also presented a damage model. Their method requires investigation of failure layer by layer. They explain reasonable damage progression results can only be achieved by conducting analysis layer by layer and increasing load incrementally to witness the all steps of failure process. Their observation is for almost all the cases the failure initiates with inter-fiber fracture (IFF) in several layers and complete failure is advanced by fiber fracture (FF) [24]. Degradation of properties after failures is applied regarding two scenarios. First scenario is the failure of a single fiber before breakage of many fibers, which results in ultimate failure of laminate. Failure of a single fiber can result in debonding of fibers with matrix and formation of micro cracks in matrix medium. This causes a reduction in fracture resistance, which determines inter-fiber failure. Hence the first degradation is done in fracture resistances by a weakening factor. Second scenario is for increased crack density. In this case transverse stiffness shall be reduced. For the case of opening cracks, secant moduli E_{2s}, G_{21s} and Poisson's ratio v_{12} is decreased with a factor η. A gradual degradation in stiffness is recommended after the onset of damage. Furthermore, a selective degradation for the cases $\sigma_2 < 0$ is advised. They also pointed out the application of load shall be in small increments after the failure of first ply, but up to this load employing only one large load step is advised. On the other hand if the stress-strain curve is to be determined, then load shall be increased in small increments also until the onset of damage [25].

Bogetti et al. suggested an important study: employing a three dimensional approach, the effects in thickness direction is accounted for. Hence, the method can be utilized in the analysis of thick laminates. Maximum strain failure criterion is adopted for failure check for the progressive failure analysis. When failure of a lamina takes place, the modulus and Poisson's ratio affecting the failure mode is diminished to an insignificant value [26].

Satyanarayana et al. [23] have presented good predictions for net-shear, pull-out and delamination modes of laminate having a hole by employing a progressive failure analysis. They investigated the failure of carbon-epoxy laminates in quasi-isotropic configuration and under tension. Both inter-laminar and intra-laminar failures were regarded to identify the above-mentioned modes. The idea for conducting the analysis following this way was in fact developed in previous studies [31, 32] the author Satyanarayana had also participated in. First study in 2006, a 2D analysis considering only intra-laminar damages, revealed without delamination modeling path of damage and failure load cannot be obtained correctly. Second study in 2007, the mode and load of failure was predicted firstly just considering the intra-laminar damages and then regarding both intra- and inter-laminar damages and finally the results from these analyses were checked against experimental findings. It was concluded that predictions are more compatible with the experimental results utilizing the model regarding both in-plane failures and delamination; as delamination changes the mode of damage especially around hole and may lead to wrong predictions when not taken into account. The suggested methodology in that was totally applied in the following study: a 3D

progressive analysis model utilizing the user-written VUMAT subroutine of ABAQUS™ Explicit nonlinear solver was constructed. Hashin-Rotem criteria, differentiating between fiber and matrix modes for in-plane damages, and cohesive zone method for inter-laminar damages were performed. When a failure is observed in matrix material, the transverse and shear stresses are diminished and in case of a fiber failure all the axial, transverse and shear stresses are diminished. The failure condition for matrix material is strain in transverse or shear direction approaches 25%. The degradation was rapidly applied, called as ply-degradation. Additionally, the effect of Poisson's ratio was not considered after the failure of matrix and transverse and shear stresses were zeroized. Failed elements are deleted from the model and the analysis continues without them. Despite, this type of degradation is not recommended in many of the studies because of the induced convergence problems and does not seen realistic, Satyanarayana et al. achieved to introduce well-matched results with experiments of Green et al. [33] for net-shear, pull-out and delamination failures of open-hole laminate.

2.4. Evaluation of Failure Models and Failure Criteria

Failure prediction of composite structures is an issue that has been tried to be solved from the very first applications of composite materials; however there is still a lack of reliable methods. A committee from UK, gathered originators of different failure prediction methodologies to solve this problem and an important study, World Wide Failure Exercise (WWFE), was performed. The aim of WWFE is to find a general method or a set of methods that can give satisfactory estimations of the failure behavior of a broad range of laminates and loading conditions. In the study, the predictions of nineteen failure criteria were compared; furthermore fourteen test cases were generated and experimental results gathered compared with the results from the failure criteria [34]. The comparison cases include failure of unidirectional lamina under biaxial loading, initial and final failure guesses for multi-directional laminates under biaxial loading and stress-strain curve obtainment under uniaxial and biaxial loading conditions [35]. Within the exercise, originators also presented the weaknesses of their methods and the ways to use it more effectively [36].

A set of very significant facts are pointed out by WWFE. First of all, the use of most of the methods are only limited to the cases they based on. When the cases which were not considered in the derivations are predicted, even for simple conditions i.e. unidirectional laminate experiencing in-plane loading, the predictions of current failure criteria can have deviations from experimental results and the method becomes unreliable. For instance, the methods of Hart -Smith were developed based on the experience in aerospace industry where only fiber failure and stiffness effects are important, no effect of matrix failure is considered. Thus, although it can yield very accurate results for some specific laminate design configurations, except for these cases the method remains weak [34, 37]. Being aware of this deficiency, Pinho et al. [38] developed three-dimensional failure criteria for each main failure mode (delamination, matrix compression, fiber compression, matrix tensile and fiber tensile failures) for laminated FRP by modifying various failure criteria in literature. That criteria set are called as LaRC04. Results from LaRC04 checked against experimental results for a wide spectrum of load cases (including three-dimensional loading conditions) to verify the criteria and the authors concluded that their criteria yields better predictions than most of the commonly used criteria. They defend the success of their criteria is a consequence of physical models constructed for each mode of failure. These well-established models can interpret failure mechanism and envelope with high accuracy. However, they also pointed out that failure process of composite materials could not be totally explored yet and that is the main reason of deviations of all the present criteria. Hence, it is crucial to be aware of the bounds and capabilities of criteria used before applying it.

Another fact deduced in WWFE, modeling and estimating the final failure strength is a very complex issue since nonlinearities are developed after the onset of damage, i.e. fibers alignment changes [39].

In analyzing composite laminates, two approaches can be followed: meso-modeling and micro modeling. In meso modeling, the properties obtained from tests of a lamina are used to evaluate the behavior of a complete laminate. In micro modeling, first the properties of the lamina are calculated based on the experimental data of the properties of the fibers and the matrix materials, and then the laminate and lastly the structural properties are assessed. If effectively applied, with micro modeling, the outcome of material changes can be evaluated. However, extra calculations that the method requires can result in placing extra inaccuracies to property calculations. And most probably, the latter was the case that the originators, Chamis [40], Mayes [41] and Huang [42] came up with. The accuracies of laminate properties of calculated with their methods were ranked in the middle within all the methods used. Another approach followed by a number of originators was to use only some micro-mechanics in their methods [37].

The accuracy of the methods was tested in various aspects and findings of the WWFE indicated that the best methods that can predict failure: Zinoviev [43], Bogetti [26], Puck [24, 25] , Cuntze [30, 44] and Tsai (Tsai-Wu) [45, 46]. The naming of the criteria here is given by only taking the name of first author conducting the study for shortening. Puck and Cuntze have the highest accuracy in most of the cases, while Bogetti's approach having the highest number of insignificant weaknesses among all. Except Zinoviev, all the aforementioned methods consider a three-dimensional state of stress. Actually, Tsai and Cuntze developed a 2D method initially, but turned to 3D for better approximations after comparison with experimental results. For failure evaluation only for one lamina, Tsai's failure criterion gives the best results, followed by Cuntze-B (the "-*B*" stands for the modified version of the method after comparison with the experimental results) and Puck (see Figure 2.3). For the estimation of initial failure strength of multidirectional laminates, Bogetti and Zinoviev work well but since residual thermal stresses are not taken into account in their methods, they cannot be definitely recommended. For final collapse of multidirectional laminates, shown in Figure 2.4, none of the theories can give results with 10% accuracy in 40% of the investigated cases; they all overestimated the strength. Still, Puck and Cuntze followed by Zinoviev, Tsai-B is recommended to be used for final failure strength estimation. For deformations, Zinoviev yields the best estimations, however Puck is better if material nonlinearity will be taken into account at moderate strains. Besides, Puck gives acceptable predictions for the mode of lamina and laminate failure [34, 37, 39].
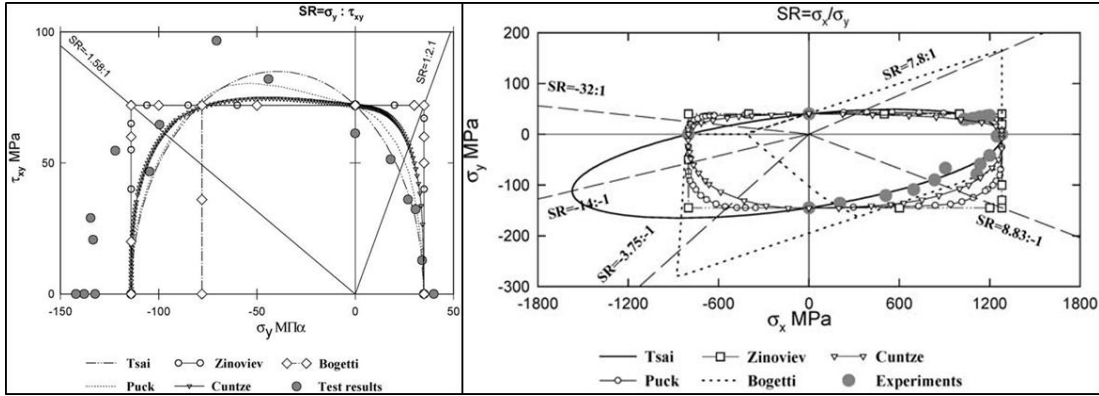
Figure 2.3 Comparison of recommended method predictions and experiments for failure stress of a UD fibre-reinforced glass lamina under combined loading [37].
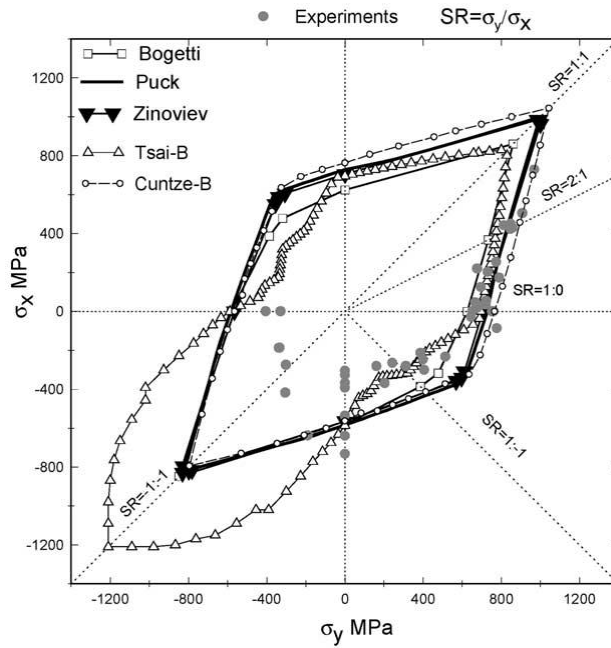
Figure 2.4 Comparison of final strength predictions and experiments of a quasi-isotropic AS4/3501-6 laminate [37].

Among the above mentioned recommended methods the formulation of Tsai-Wu and Puck were depicted in previous sections. Tsai's method presented in WWFE presumes material properties are linear elastic until the initiation of failure and the stiffness is degraded after then. Puck employs a three-dimensional, non-linear progressive failure approach. Cuntze's method also takes into account three-dimensional stress state since it originates from Puck's, and similarly the method works by checking failure modes. The difference is in taking

into consideration of the interaction between modes [39]. In Cuntze's method, named as failure mode concept (FMC), the complete failure surface is constituted piecewise smoothly by partial failure surfaces. At each partial failure surface only one failure mechanism can be active. Moreover, for each mode there is a fundamental strength defined. In addition to these, a scalar failure potential for each mode can be obtained by employing the homogenized material properties calculated utilizing the material symmetries of the lamina [44].

Zinoviev et al. [43] applied maximum stress criterion in their method and material properties are considered to be linear-elastic until initial failure. The approach making this method strong is that after the onset of damage, the altering of the directions of the fibers is taken into account. Bogetti [26] introduced a three-dimensional method utilizing maximum strain criterion and ply modulus discount method for progressive failure approach and predicted good results for final failure strength and initial part of the stress-strain curves of laminates [39].

At the end of WWFE it is concluded that some issues important for the prediction of failure can be solved by the theoreticians; however there are still very important cases to be explained. The following table portrays the capabilities of the methods in literature and the issues that are either cannot be solved or not taken into account in scope of this study, so to be dealt with [37].

Table 2.1 Conclusion of WWFE on issues solved and to be dealt with for prediction of failure [37].

Issues solved	Issues to be dealt with
Micro-mechanics approach for predictions	Taking into account thermal residual stress
Isolated lamina under biaxial loads	Multiple material and structural non-linearities
Failure mode detection	Thick and thin laminate
Failure envelope production for a laminate	Lay-up sequence consideration
Single material non-linearity	Large deformation prediction
Post failure modeling	Three-dimensional failure criteria
	Delamination
	Environmental factors

Knight developed a user-defined material model (UMAT) and inserted it in the commercial finite element analysis tool ABAQUS to examine the effects of implying different failure criteria in a progressive failure analysis. Maximum stress, maximum strain, Tsai-Wu and Hashin criteria were compared for the initial failure calculation. The material properties were degraded by using ply-discount method. In the study both two dimensional and three dimensional analyses were performed [8].

Puck and Schürmann [25] claimed achieving results reflecting physical reality from the analysis of FRP laminates, the nonlinearity of the stress-strain relationships shall be regarded and an appropriate fracture criteria with a suitable degradation model shall be

applied. The fracture criteria should differentiate between the failure modes, such as fiber and inter-fiber failures. Consideration of failure mode results in more accurate stress estimations and detection of crack direction. Crack direction information may be used to explore the reasons of complete fracture. Puck and Schürmann explained that there are only a few fracture criteria and degradation models which can be easily implemented while giving realistic results; and one of these methods is suggested by them [25].

For a model constructed to simulate four-point-bending test a comparison was made between the Tsai and Hashin failure criteria. Both was found to be appropriate, however use of Hashin was suggested since it can predict the failure modes as well, it catches failures better than Tsai [14].

In real world, in composite materials, the failure develops in the matrix and in the fiber separately in a discrete and non-continuous way. Thus, in contrast to what is made in most of the failure criteria mentioned above, the material represents nonlinear properties. However, most of the presented criteria presume the material as homogeneous and linear elastic, which will cause convergence problems and wrong results. Hence, considering the material nonlinearity with a micromechanics based approach is advisable to achieve accurate results [47].

Bogetti et al. advocates that even the most sophisticated methods are not capable of simulating the failure of laminates for a diverse material, lay-up and loading combinations; hence no universally valid failure analysis exist [48].

2.5. A Review of Literature in Comparison with the Procedures of This Study

Reviewing the literature, it is concluded that great efforts have been made predicting the failure of composite structures. In this study, a successful progressive failure analysis approach including the choice of appropriate failure criterion is investigated. A summary of recommended methods from literature for a good prediction of failure and an in-depth comparison of these with the method employed in this study is given in this section.

There are various ways of implementing progressive failure analysis. The differences can be in the calculation of strains and stresses, controlling for failure, reduction of material properties and monitoring the behavior after property degradation. The aim of this study is to reach the best prediction of failure exploiting the right method.

Progressive failure analysis initiates with the assessment of the strains and stresses in the structure. The variance between different applications of the method also starts with the calculation of these tensors. For instance, elasticity of the material is one of the reasons of dissimilar results. In Marc® property of material is taken as linear elastic until failure starts; however, there are academic work suggesting introduction of nonlinear material properties for a better prediction of failure [25, 26, 28, 49].

Following step is failure check introducing the calculated stresses or strains in failure criterion. Choice of the failure criterion is another cause of variance between methods of progressive failure analysis. Some methods care for failure process and predicts for mode of failure; but some only define an envelope that the part can operate safely within. Failure criteria can be split into two groups in this aspect as mode dependent and mode independent. The Hashin and the Puck criteria utilized in this study are mode-dependent, whereas the Tsai-Wu criterion is mode independent. The maximum stress and the maximum strain criteria analyze the direction of failure. Most of the studies in literature suggest that the more is known on the mode of failure the better predictions can be made. It is also declared that all the failure criteria give the best results for the loading and the lamination cases they are derived for. In this study, both mode dependent and mode independent criteria are investigated and the results of them are compared.

Next step of the progressive failure analysis is the degradation of the material properties of the elements that the failure indices become larger than one. In some studies, the properties are reduced suddenly to none. Some studies derived formulations or constants special to every failure mode for this reduction process. Another commonly used approach is decreasing the properties to 10% of the original value. In addition to these, there are studies applying different procedures for the reduction of the elastic constants and the Poisson's ratios. In this study, the gradual selective degradation method is chosen. There are many sources claiming that this method is both more realistic and causes fewer problems among all.

The last difference can be in the procedure followed after degradation. For most of the simulations, the load causing the failure at the current step is reapplied to the structure to check whether additional failures are obtained after reduction or not. However, some studies skip the evaluation with the same loading and continue with the next load increment. The idea behind is that in progressive failure analysis, the load increment is usually very small and it would not cause a large error to neglect the estimation with the same loading. Consequently, the run-time will be shorter. However, for this study the strains and stresses are re-calculated after diminution.

Each of the aforementioned variances can result in completely different outcomes since the progressive failure analysis is too sensitive to changes in conditions. The most suggested practices of literature are tried to be followed in this study to reach a good prediction.

CHAPTER 3

THEORETICAL BACKGROUND

3.1. Introduction

For failure analysis of composite structures, the basics of mechanics of composite materials and failure prediction methods are to be known. Descriptions of these subjects are presented in this chapter as needed in scope of this study.

3.2. Mechanics of Composite Materials [5, 50]

Composite materials are heterogeneous and anisotropic; which means the properties within the material differ with respect to position and the properties at a point depends on the direction. Due to the inhomogeneous characteristics of composite materials their mechanical behavior can be investigated in both micro and macro scale. In micromechanics approach, in order to explore the properties of composite material the interaction of its constituents are examined in microscopic scale. Whereas, in macromechanics the properties of constituents are not taken into account separately, an average property is found that can present the main characteristic of the resultant material and this property is assumed to be homogeneously distributed. For structural analysis macromechanics is more commonly used.

3.2.1. Constitutive Relations

Let the fiber reinforced composite material is linearly elastic. Then, generalized Hooke's law is applicable:

$$\sigma_i = C_{ij}\varepsilon_j \qquad\qquad i,j = 1,2,\dots,6 \tag{3.1}$$

Because of the symmetry of the stiffness matrix, C_{ij}, for anisotropic materials, it has 21 independent constants instead of 36 constants. When symmetry of material property exists with respect to two orthogonal planes, the property is also symmetric with respect to a third mutually orthogonal plane. This type of material is called as orthotropic material and for orthotropic materials number of independent stiffness components reduces to 9. The lamina of a fiber reinforced composite is assumed to be orthotropic. The stress-strain relationship for an orthotropic lamina can be written as;

$$
\begin{Bmatrix} \sigma_1 \\ \sigma_2 \\ \sigma_3 \\ \tau_{23} \\ \tau_{13} \\ \tau_{12} \end{Bmatrix}
=
\begin{bmatrix}
C_{11} & C_{12} & C_{13} & 0 & 0 & 0 \\
C_{12} & C_{22} & C_{23} & 0 & 0 & 0 \\
C_{13} & C_{23} & C_{33} & 0 & 0 & 0 \\
0 & 0 & 0 & C_{44} & 0 & 0 \\
0 & 0 & 0 & 0 & C_{55} & 0 \\
0 & 0 & 0 & 0 & 0 & C_{55}
\end{bmatrix}
\begin{Bmatrix} \varepsilon_1 \\ \varepsilon_2 \\ \varepsilon_3 \\ \gamma_{23} \\ \gamma_{13} \\ \gamma_{12} \end{Bmatrix}
\tag{3.2}
$$

As can be seen from the relationship, for an orthotropic lamina, normal stresses are not affected by shear strains; similar relationship is also true for shear stresses and normal strains. Thus, for orthotropic lamina, extension-shear coupling is not observed. Still, if loading is in a non-principle direction, then the output deformation obviously becomes anisotropic [5].

The non-zero components of the stiffness matrix can be obtained by utilizing the formulae

$$C_{11} = \frac{1 - \nu_{23}\nu_{32}}{E_2 E_3 \Delta} \qquad C_{12} = \frac{\nu_{21} - \nu_{31}\nu_{23}}{E_2 E_3 \Delta} = \frac{\nu_{12} - \nu_{32}\nu_{13}}{E_1 E_3 \Delta}$$

$$C_{22} = \frac{1 - \nu_{31}\nu_{13}}{E_1 E_3 \Delta} \qquad C_{23} = \frac{\nu_{32} - \nu_{12}\nu_{31}}{E_1 E_3 \Delta} = \frac{\nu_{23} - \nu_{21}\nu_{13}}{E_1 E_2 \Delta}$$

$$C_{33} = \frac{1 - \nu_{12}\nu_{21}}{E_1 E_2 \Delta} \qquad C_{13} = \frac{\nu_{31} - \nu_{21}\nu_{32}}{E_2 E_3 \Delta} = \frac{\nu_{13} - \nu_{12}\nu_{23}}{E_1 E_2 \Delta}$$

$$C_{44} = G_{23} \qquad C_{55} = G_{31} \qquad C_{66} = G_{12} \tag{3.3}$$

where

$$\Delta = \frac{1 - \nu_{12}\nu_{21} - \nu_{23}\nu_{32} - \nu_{31}\nu_{13} - 2\nu_{21}\nu_{32}\nu_{13}}{E_1 E_2 E_3} \tag{3.4}$$

3.3. Failure Criteria

Failure criteria are the methods developed for exploring whether the composite structure can sustain safely the operation loads or not. Most of the experiments to obtain strength a composite are only executed for a uniaxial state of stress while most of the real world applications require a control for a multi-axial stress-state. However, it is neither practical nor possible to conduct experiments for all the possible orientations of the composite for all possible loading conditions. Hence, methods are needed to use available data of uniaxial measurements to obtain failure under other conditions [5]. Failure criteria are proposed to make possible the examination of the complex failure behavior of composite materials in ply level with this limited information. In this section, descriptions and formulations of these criteria are presented.

Some of the failure criteria take into account the mode of failure. This information is important in progressive damage analysis since the property to be degraded pointed directly. The modes of failure that some criteria examined separately are delamination, matrix compression failure, fiber compression failure, matrix tensile failure and fiber tensile failure.

3.3.1. Maximum Stress Failure Criterion

Maximum stress failure criterion is mode-independent. Furthermore, it does not take into account the interactions between the failure modes; each equation checks failure like an independent criterion.

According to maximum stress failure criterion, if the stress in a principle direction is higher than respective strength, then the lamina is said to be failed. For an intact lamina the following conditions shall be satisfied [5].

$$\sigma_1 < X_t \text{ if } \sigma_1 > 0 \qquad\qquad \sigma_1 > X_c \text{ if } \sigma_1 < 0 \tag{3.5}$$

$$\sigma_2 < Y_t \text{ if } \sigma_2 > 0 \qquad\qquad \sigma_2 > Y_c \text{ if } \sigma_2 < 0 \tag{3.6}$$

$$\sigma_3 < Z_t \text{ if } \sigma_3 > 0 \qquad\qquad \sigma_3 > Z_c \text{ if } \sigma_3 < 0 \tag{3.7}$$

$$|\sigma_{12}| < S_{12} \tag{3.8}$$

$$|\sigma_{23}| < S_{23} \tag{3.9}$$

$$|\sigma_{13}| < S_{13} \tag{3.10}$$

3.3.2. Maximum Strain Failure Criterion

Like in the maximum stress criterion the inequalities shall be satisfied for no failure and there is no interaction between the modes of failure.

$$\varepsilon_1 < e_{1t} \text{ if } \varepsilon_1 > 0 \qquad\qquad \varepsilon_1 > e_{1c} \text{ if } \varepsilon_1 < 0 \tag{3.11}$$

$$\varepsilon_2 < e_{2t} \text{ if } \varepsilon_2 > 0 \qquad\qquad \varepsilon_2 > e_{2c} \text{ if } \varepsilon_2 < 0 \tag{3.12}$$

$$\varepsilon_3 < e_{3t} \text{ if } \varepsilon_3 > 0 \qquad\qquad \varepsilon_3 > e_{3c} \text{ if } \varepsilon_3 < 0 \tag{3.13}$$

$$|\gamma_{23}| < g_{23} \tag{3.14}$$

$$|\gamma_{13}| < g_{13} \tag{3.15}$$

$$|\gamma_{12}| < g_{12} \tag{3.16}$$

3.3.3. Tsai-Wu Failure Criterion

A quadratic failure criterion, taking into account the interaction of stress components is suggested by Tsai-Wu. The mode of failure cannot be differentiated by the criterion.

The interactions of stresses are established by interaction constants. For instance, F_{12} relates normal stresses σ_1 and σ_2.

Failure index is calculated with the formula,

$$\begin{aligned}
FI = \Bigg[&\left(\frac{1}{X_t} - \frac{1}{X_c}\right)\sigma_1 + \left(\frac{1}{Y_t} - \frac{1}{Y_c}\right)\sigma_2 + \left(\frac{1}{Z_t} - \frac{1}{Z_c}\right)\sigma_3 + \frac{\sigma_1^2}{X_t X_c} + \frac{\sigma_2^2}{Y_t Y_c} + \frac{\sigma_3^2}{Z_t Z_c} + \frac{\tau_{12}^2}{S_{12}^2} + \frac{\tau_{23}^2}{S_{23}^2} \\
&+ \frac{\tau_{13}^2}{S_{13}^2} + 2F_{12}\sigma_1\sigma_2 + 2F_{23}\sigma_2\sigma_3 + 2F_{13}\sigma_1\sigma_3 \Bigg]
\end{aligned}$$

$$\tag{3.17}$$

F_{12} : Interactive stress constant for plane 12

F_{23} : Interactive stress constant for plane 23

F_{13} : Interactive stress constant for plane 31

3.3.4. Hashin Failure Criterion

Considers failures of matrix and fiber separately, and additionally failure in tension and compression of these also examined separately.

Tension fiber mode;

$$\left(\frac{\sigma_{11}}{X_t}\right)^2 + \frac{1}{S^2}(\sigma_{12}^2 + \sigma_{13}^2) = 1$$

Or

$$\sigma_{11} = X_T$$

(3.18)

Compressive fiber mode; $\sigma_1 < 0$

$$\frac{|\sigma_{11}|}{X_c} = 1$$

(3.19)

Tensile Matrix Mode; $\sigma_2 + \sigma_3 > 0$

$$FI = \left[\frac{1}{Y_t}(\sigma_2 + \sigma_3)^2 + \frac{1}{S_{23}^2}(\sigma_{23}^2 + \sigma_2\sigma_3) + \frac{1}{S_{12}}(\sigma_{12}^2 + \sigma_{13}^2)\right]$$

(3.20)

Compressive matrix mode; $\sigma_2 + \sigma_3 < 0$

$$FI = \left[\frac{1}{Y_c}\left(\left(\frac{Y_c}{2S_{23}}\right)^2 - 1\right)(\sigma_2 + \sigma_3) + \frac{1}{4S_{23}^2}(\sigma_2 + \sigma_3)^2 + \frac{1}{S_{23}^2}(\sigma_{23}^2 + \sigma_2\sigma_3)\right.$$
$$\left. + \frac{1}{S_{12}^2}(\sigma_{12}^2 + \sigma_{13}^2)\right]$$

(3.21)

3.3.5. Puck Failure Criterion

Puck failure criterion employs distinct fracture criteria for fiber failure (FF) and inter-fiber failure (IFF). Nonetheless, the main advantage it provides is making possible to identify the mode of failure [25, 49]. (The term inter-fiber failure describes both the cracks formed due to cohesive matrix failure and the cracks advancing through entire thickness –no visible failure- but cannot move across the fibers of adjacent fibers. [24])

The fiber and matrix failures are treated separately also in the Hashin's criteria. Different from Hashin, Puck assesses fracture failure angle for matrix failure (see Figure 3.1). Fracture caused by matrix failure will take place at this angle [49].
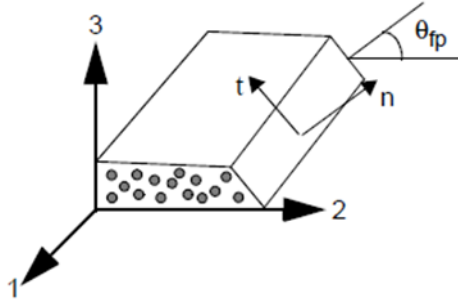
n: fracture plane normal direction
t: fracture plane tangential direction
θ_{fp}: Fracture failure angle

Figure 3.1 Fracture failure angle and preferred coordinate [49].

Tests of carbon fiber and glass fiber laminates explored the brittle fracture characteristic of unidirectional plies. Until the failure load no definite sign of plastic deformation is monitored and when that load is reached material ruptures suddenly. This behavior is obvious especially for the inter-fiber failure mode. Considering this, Puck and Schürmann criticizes the approaches developed depending on the yield criteria of von Mises and Hill which can only give meaningful results in case of ductile material behavior. Instead, they defended following Mohr's hypotheses is more suitable developing a failure criteria. This idea was actually stated by Hashin previously. However, the application is developed by Puck and have accomplished satisfactory predictions for the inter-fiber failure mode [25].

For fiber failure (FF):

Tensile fiber mode, $\sigma_1 > 0$

$$FI = \frac{\sigma_1}{X_t} \tag{3.22}$$

Compressive fiber mode, $\sigma_1 < 0$

$$FI = \frac{|\sigma_1|}{X_c} \tag{3.23}$$

The calculation of inter-fiber failure is more complicated. The relations are constituted following Mohr's method as stated already; hence, the cause of failure is considered as the stresses only on failure plane. Thus, the stresses in material coordinates are transformed to failure plane firstly.

$$\sigma_n = \sigma_2 \cos^2 \theta + \sigma_3 \sin^2 \theta + 2\sigma_{23} \sin \theta \cos \theta \tag{3.24}$$

$$\sigma_{nt} = (\sigma_3 - \sigma_2) \sin \theta \cos \theta + \sigma_{23}(\cos^2 \theta - \sin^2 \theta) \tag{3.25}$$

$$\sigma_{nl} = \sigma_{31} \sin \theta + \sigma_{12} \cos \theta \tag{3.26}$$

A failure condition dependent on θ can now be written. An important point before writing such a failure condition is consideration of the effect of normal stress on fracture plane. If this stress is tensile, it helps fracture. On the other hand, when compressive, it obstructs shear

21

fracture. For $\sigma_n < 0$, for fracture, shear stresses on failure plane shall overcome extra resistance which is created by σ_n and increasing with the value of σ_n. This mechanism is like internal friction, hence the formulations are inspired by Mohr-Coulomb [25].

For inter-fiber failure (IFF) [49]:

For $\sigma_n \geq 0$

$$f(\theta) = \sqrt{\left(\frac{1}{Y_t} - p_1\right)^2 \sigma_n{}^2 + \left(\frac{\sigma_{nt}}{R^A}\right)^2 + \left(\frac{\sigma_{nl}}{S_{12}}\right)^2} + p_1 \sigma_n \tag{3.27}$$

For $\sigma_n < 0$

$$f(\theta) = \sqrt{\left(\frac{\sigma_{nt}}{R^A}\right)^2 + \left(\frac{\sigma_{nl}}{S_{12}}\right)^2 (p_2 \sigma_n)^2} + p_2 \sigma_n \tag{3.28}$$

where

$$p_1 = \frac{p_{\perp\perp}^{(+)}}{R^A} \frac{\sigma_{nt}^2}{\sigma_{nt}^2 + \sigma_{nl}^2} + \frac{p_{\perp\parallel}^{(+)}}{S_{12}} \frac{\sigma_{nl}^2}{\sigma_{nt}^2 + \sigma_{nl}^2} \tag{3.29}$$

$$p_2 = \frac{p_{\perp\perp}^{(-)}}{R^A} \frac{\sigma_{nt}^2}{\sigma_{nt}^2 + \sigma_{nl}^2} + \frac{p_{\perp\parallel}^{(-)}}{S_{12}} \frac{\sigma_{nl}^2}{\sigma_{nt}^2 + \sigma_{nl}^2} \tag{3.30}$$

Utilizing the equations (3.24) through (3.30) and knowing θ values is between -90 and 90 degrees, the critical failure angle, θ_{fp} is estimated by numerical methods.

The following formulae are used for the calculations above:

$$R^A = \frac{Y_c}{2\left(1 + p_{\perp\perp}^{(-)}\right)} = \frac{S_{12}}{2p_{\perp\parallel}^{(-)}}\left(\sqrt{1 + 2p_{\perp\parallel}^{(-)} \frac{Y_c}{S_{12}}} - 1\right) \tag{3.31}$$

$$\sigma_{21c} = S_{12}\sqrt{1 + 2p_{\perp\perp}^{(-)}} \tag{3.32}$$

Where,

σ_n : Normal stress on the potential fracture plane

τ_{nl}: Shear stress on potential fracture plane along fiber longitudinal direction

τ_{nt}: Shear stress on potential fracture plane along fiber transverse direction

$p_{\perp\parallel}^{(-)}$: Slope of the (σ_n, τ_{nl}) fracture envelope for σ_n. 0 For $\sigma_n = 0$

$p_{\perp\perp}^{(-)}$: Slope of the (σ_n, τ_{nt}) fracture envelope for σ_n. 0 For $\sigma_n = 0$

R^A: Fracture resistance of a stress action plane

The mode of failure predicted following Puck's approach give even more data on failure than experimental results for the plane stress case. The predictions give the angle of fracture plane, which is used to evaluate the possibility of delamination and local buckling. These failure modes occurs owing to wedge effect happening as a result of high compressive transverse stress on oblique failure plane [24].

CHAPTER 4

NUMERICAL AND EXPERIMENTAL PROCEDURES

In this study, the target is to suggest numerical analysis methods to examine a thick cross-sectioned composite structure. The compatibility of these methods is then verified by tests. This chapter is devoted to description of procedures followed to achieve these goals. The structure of interest is defined firstly, and then the details of numerical analyses and experimental processes are presented.

4.1. Description of Analyzed Structure

The assembly shown in Figure 4.1 is constructed and investigated in scope of this work.

The main parts of the assembly are an approximately 35 mm thick composite laminate and steel bushings. The laminate has a hybrid composition, made up of carbon fabric layers, glass layers and foam. Four holes are drilled on this structure. Holes 1 and 2 (see Figure 4.1) are for examining bolted connection effect to the laminate and have interference fit bushings mounted in them. Holes 3 and 4 are just for fastening the composite to a grip (grip 2) which enables the connection of the part to the tension test machine. In the same vein, another grip (grip 1) bolted to holes 1 and 2. These parts can be changed with other parts in some of the tests. A more detailed definition of these assemblies is presented in Section 4.3. In order to prevent any damage during tests that can be caused by the contact of the grip 1 to composite, a hard, plastic-like material (named as spacer) is bonded to the top and bottom surfaces of the composite. There are two more auxiliary parts (reinforcement parts) utilized in the assembly with the purpose of reinforcing the part of composite that the load is applied. All the parts of the assembly use are listed in the Table 4.1 and depicted in Figure 4.1.
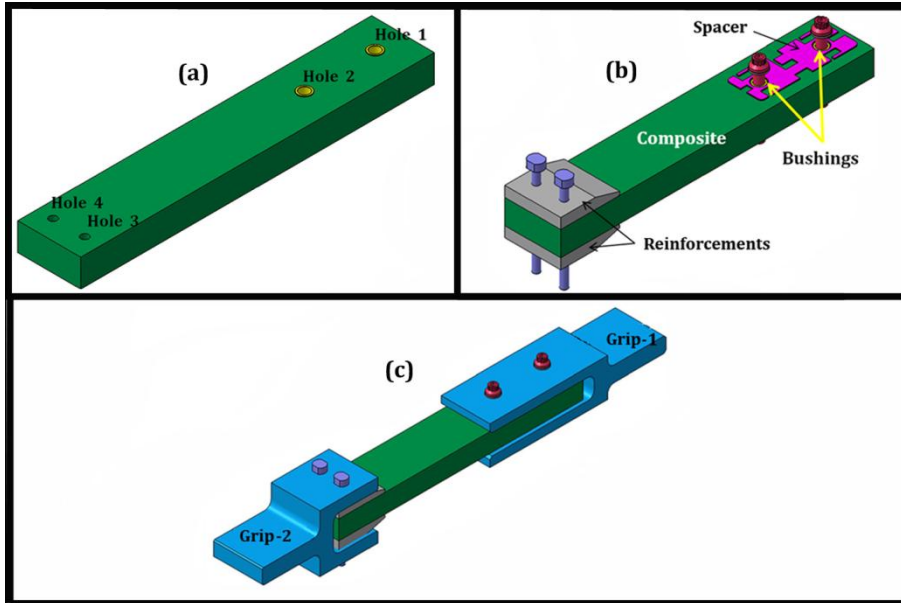
Figure 4.1 The analyzed structure.

Table 4.1 Part list of the assembly

Part description	# in assembly
Composite laminate	1
Bushing	2
Bolts (1 and 2)*	2
Bolts (3 and 4)*	2
Grip-1	1
Grip-2	1
Spacer	2
Reinforcement	2
Bolts and bushings take the number of the corresponding hole (see Figure 4.1 for hole numbering)	

4.1.1. Geometric Dimensions

The dimensions of the analyzed parts are displayed in Figure 4.2 and the nominal dimensions of the bolts and bushings are given Table 4.2.
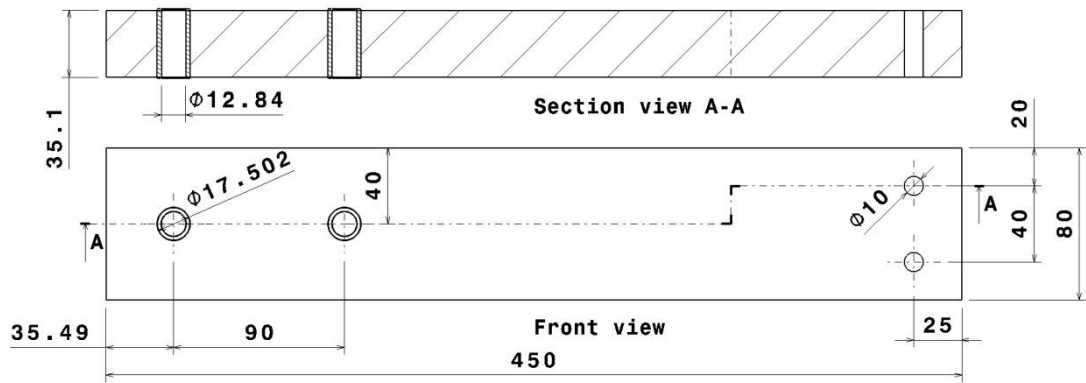
Figure 4.2 Dimensions of analyzed parts.

Table 4.2 Nominal dimensions of bolts and bushings

Part description	inner diameter [mm]	outer diameter [mm]
Bushings	12.836	17.502
Bolts (1&2)	-	12.675
Bolts (3&4)	-	10

4.1.2. Material Properties

Except for the composite laminate, all the components of the assembly are made of steel. For the steels, in addition to elastic properties, plastic properties are defined considering the high local strains that may occur during testing. When the true stress-strain curve cannot be found, the following equations are utilized to convert engineering stress and strains to true stress and strains.

$$\varepsilon_{true} = \ln(1 + \varepsilon_{eng})$$

(4.1)

$$\sigma_{true} = \sigma_{eng}.(1 + \varepsilon_{eng})$$

(4.2)

4.1.2.1. The Laminate

The thick composite is formed by laminating unidirectional glass and carbon fabric prepregs by hand lay-up. Lay-up is symmetric with respect to the foam structure that is in the middle of the laminate.

Table 4.3 Lay-up description

Lay-up
$[45_{8C}/(0_C/45_C)_8/(45_C/0_C)_8/0_{20G}/45_{4C}/\text{Foam}]_s{}^{*}$
"G" and "C" subscripts imply glass UD and carbon fabric laminae, respectively.

The mechanical properties of the materials used in the construction of laminate are given in the following table. The properties of carbon fabric and glass UD is obtained in hot-wet conditions. All the data presented below is normalized based on carbon fabric properties, i.e. the property after the division symbol is always for carbon fabric.

Table 4.4 Mechanical properties of prepregs (hot-wet condition) and foam

Carbon fabric			S2 glass uni-directional		
cured ply thickness: 0.218 mm			cured ply thickness: 0.23 mm		
ρ_c / ρ_c : 1			ρ_g / ρ_c : 1.23		
E_1 / E_1: 1	X_t / X_t: 1	e_{1t} / e_{1t}: 1	E_1 / E_1 : 1.32	X_t / X_t: 1.78	e_{1t} / e_{1t}: 1.25
E_2 / E_1 : 1	X_c / X_t: 0.86	e_{1c} / e_{1t}: 0.85	E_2 / E_1: 0.312	X_c / X_t: 1.259	e_{1c} / e_{1t}: 0.85
E_3 / E_1 : 0.75	Y_t / X_t: 1	e_{2t} / e_{1t}: 1	E_3 / E_1 : 0.312	Y_t / X_t: 0.035	e_{2t} / e_{1t}: 0.025
G_{12} / E_1 : 0.06	Y_c / X_t : 0.86	e_{2c} / e_{1t}: 0.85	G_{12} / E_1 : 0.075	Y_c / X_t : 0.162	e_{2c} / e_{1t}: 0.106
G_{23} / E_1 : 0.045	Z_t / X_t : 0.10	e_{3t} / e_{1t}: 0.104	G_{23} / E_1 : 0.058	Z_t / X_t : 0.035	e_{3t} / e_{1t}: 0.025
G_{31} / E_1 : 0.045	Z_c / X_t : 0.10	e_{3c} / e_{1t}: 0.104	G_{31} / E_1: 0.052	Z_c / X_t : 0.162	e_{3c} / e_{1t}: 0.106
v_{12} / v_{12} : 1	S_{xy} / X_t: 0.10	g_{12} / e_{1t}: 0.104	v_{12} / v_{12} : 4.667	S_{xy} / X_t: 0.095	g_{12} / e_{1t}: 0.067
v_{23} / v_{12} : 5	S_{yz} / X_t : 0.10	g_{23} / e_{1t}: 0.104	v_{23} / v_{12} : 0.333	S_{yz} / X_t : 0.087	g_{23} / e_{1t}: 0.061
v_{31} / v_{12} : 0.16	S_{zx} / X_t : 0.10	g_{13} / e_{1t}: 0.104	v_{31} / v_{12} : 0.25	S_{zx} / X_t : 0.087	g_{13} / e_{1t}: 0.061
Foam	ρ_f / ρ_c : 0.049	E / E_1: 2.669E-3	v / v_{12} : 5.5		

4.1.2.2. Bushings

The bushings are made from 17-4PH H1025 steel. The elastic properties and the engineering stress-strain curve used in plastic region are as follows. The stress-strain curve is converted to true stress-strain using the equations (4.1) and (4.2).

Table 4.5 Elastic properties of 17-4PH (Table 2.6.9.0 (d) of [51])

17-4PH Steel		
$\rho = 7.83\times10^{-9}$ t/mm^3	E = 196500 MPa	v = 0.27
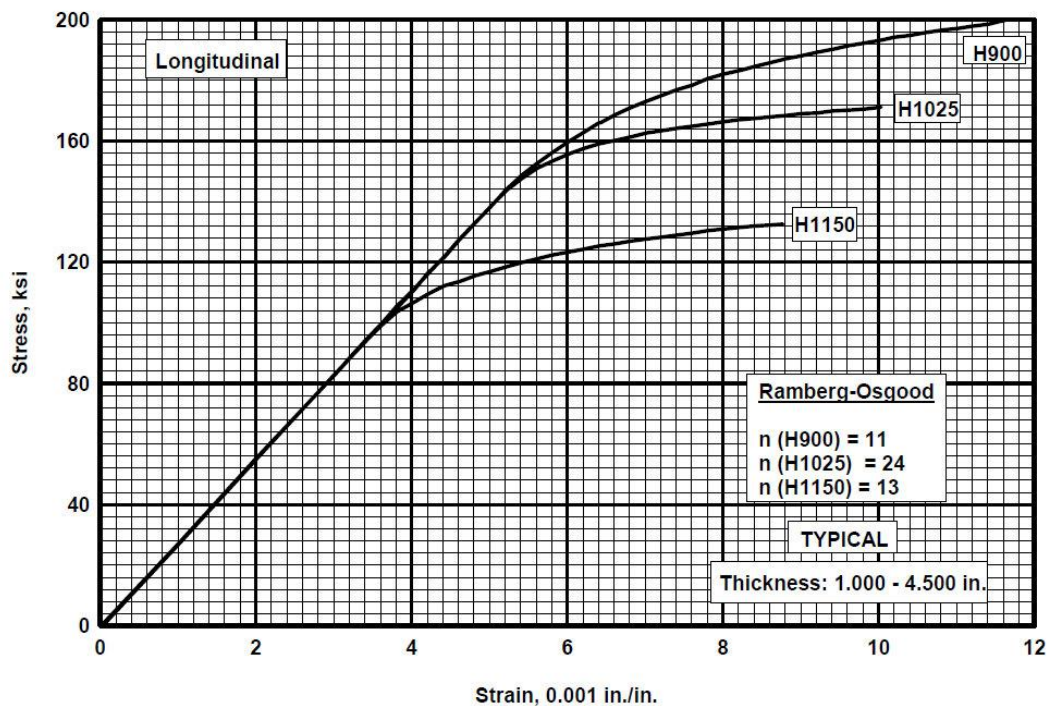
Figure 4.3 Engineering stress-strain curve for 17-4PH steel bar (Figure 2.6.9.2.6(a) of [51])

4.1.2.3. Grips

Both of the adaptors are made of AISI 4140 steel.

Table 4.6 Properties of 4140 steel

4140 Steel		
$\rho = 7.83 \times 10^{-9}$ t/mm^3	E = 200000 MPa	v = 0.30

4.2. Numerical Procedure

In scope of this study, models simulating tension test are established. Finite element analyses are conducted, the result of which are compared with the data obtained in the test. Various failure criteria are applied in the analyses and the method that is most compatible with the test results are looked for.

4.2.1. Analysis Tools

Simulations were conducted by using commercial software MSC.Mentat[®] 2010 and MSC.Marc[®] 2010. MSC.Mentat[®] is a pre- and post-processor tool enabling both constructing the model and visualizing the results; whereas MSC.Marc[®] is an implicit, nonlinear finite element analysis solver. MSC.Marc[®] has the capability of solving both static/dynamic structural problems, and coupled multi-physics phenomena problems. Moreover; MSC.Marc[®] is effective in solving contact problems including; interaction of deformable-deformable and deformable-rigid bodies, self-contact, multi-body contact, interference fit [52]. 3D-composite-modeling capability, wide element library, various non-linear solution procedures and contact preferences made this solver preferable against its alternatives for simulating the current geometry.

4.2.2. Description of the Finite Element Analysis Model

Simulations were performed by using 3D-quarter-model shown in Figure 4.4. Although, shell modeling of multi-layered materials is mostly preferred because of its computational efficiency; it is not feasible in current case due to various weaknesses it can cause. First weakness to mention is that; shell assumption of laminates yields unsatisfactory results when it is applied to thick geometries. In this case, out-of-plane-stresses (transverse normal and transverse shear) gain importance throughout the geometry, and neglecting these might cause misleading stress distribution. Hence, 3D brick modeling of thick laminates becomes essential when laminate is getting thicker. Moreover, "constant-transverse-shear through thickness" assumption during shell modeling causes incorrect stress distribution. This error is not prominent in thin structures whereas, it causes serious errors in thick structures. If shell modeling is conducted, it is not possible to track stresses and failures layer by layer accurately especially when layup is complex. In the analyzed structure of this study, in transverse direction, material orientation is continuously changing; besides, the material also changes. The cumulative effect is jumps in stress distribution through-the-thickness direction, which shall be considered.

In addition to the problems about the accuracy of stress distribution, there are some obstacles in contact detection and calculation of non-linearity in deformation through the thickness direction. Shell elements have positive and negative surfaces and thickness is specified by the positions of integration points. Therefore, displacements are gathered from 4 nodes on a bilinear topology plane. This kind of approach is not effective when (1) contact

condition is complex, (2) analysis is highly nonlinear and (3) deformations are high. Shell assumption will affect contact detection, quality and quantity of deformation. In the case of consideration, material orientation in the layers changes continuously in third direction due to large deformations, and; bending of the bolt clearly causes a non-uniform distribution of strain in transverse direction since; single- or double-lap joints both show non-uniform distribution of strain [4]. Therefore, calculation of displacement field in third direction is compulsory to be able to have accurate results.
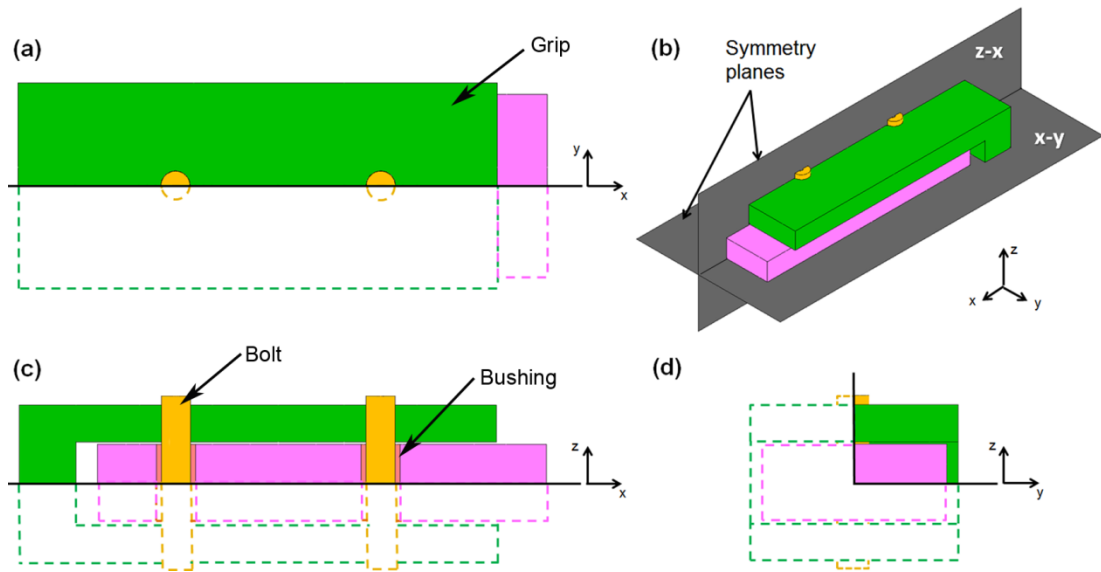
Figure 4.4 Quarter model, contact bodies and symmetry planes.

4.2.2.1. Mesh

The most appropriate approach to model composite materials through thickness is an area of research. There are studies using only one element per ply [4], more than one element per ply or multiple plies per element. In this study, the approach, proposed by Zimmermann et al. [2], namely; having more than one ply in one element is followed (Figure 4.5). For better calculation of shear stresses in ply level, the number of elements through the thickness is increased [2]. The consequences of changing number of elements through the thickness are discussed in Section 5.4.1. In the light of this investigation, the laminate is divided into six parts. The partition is done considering material and directions of the laminae. Layers showing similar material and repetitive lay-up characteristics are grouped together and they are regarded as sub-laminates. In total, there are five sub-laminates through thickness. The layer that is located at the very bottom is not considered as sub-laminate since it is made of single material foam. Numbering of sub-laminates is presented in Figure 4.6. Layer 1 -the ply at the middle of the structure- is foam, whereas other layers (2-65) are located at the sub-laminates as they are shown in the figure. The mesh of the laminate is constructed continuum composite elements. Within this element, modeling

different material properties, different thicknesses, and different orientations is allowed. A 3D composite brick element, type 149, is used to model laminate, due to its efficiency in multi-layered material analysis. Detailed information about this type of element is presented in Section 4.2.2.1.1.

Another type of element to model a composite material is to use a special type of element, called as rebar element. Rebar elements are empty elements. Uni-directional strain members are embedded in these elements. Then, the element is placed in a solid element to simulate a reinforced material, where the solid element represents the filler and the rebar element represents the reinforcing material. However, this special type of element is more suitable and efficient for modeling tires or concretes where the material is reinforced in only one direction.

Mesh of the metallic components (bushings, bolts and grip) is presented in Figure 4.5. Elements are refined near holes to improve contact detection and accuracy around high-stress-locations. Standard eight node quadrilateral element (Element type 7) is used to improve computational efficiency.
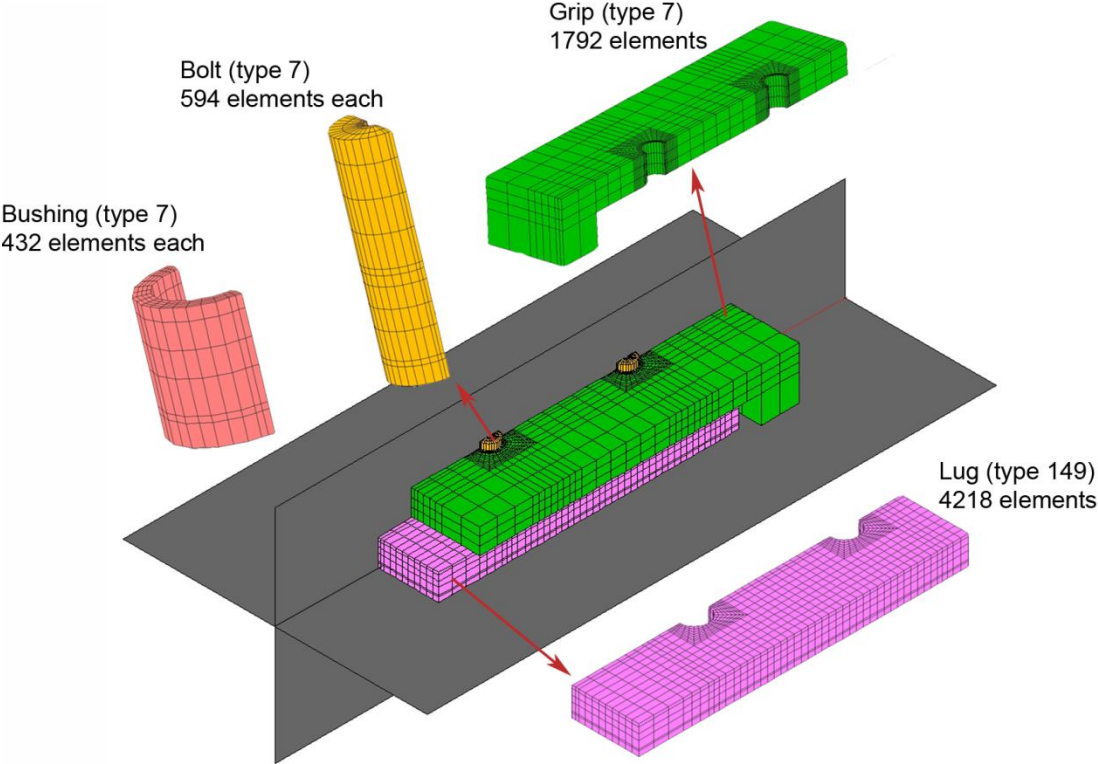
Figure 4.5 Types of the elements used in modeling.
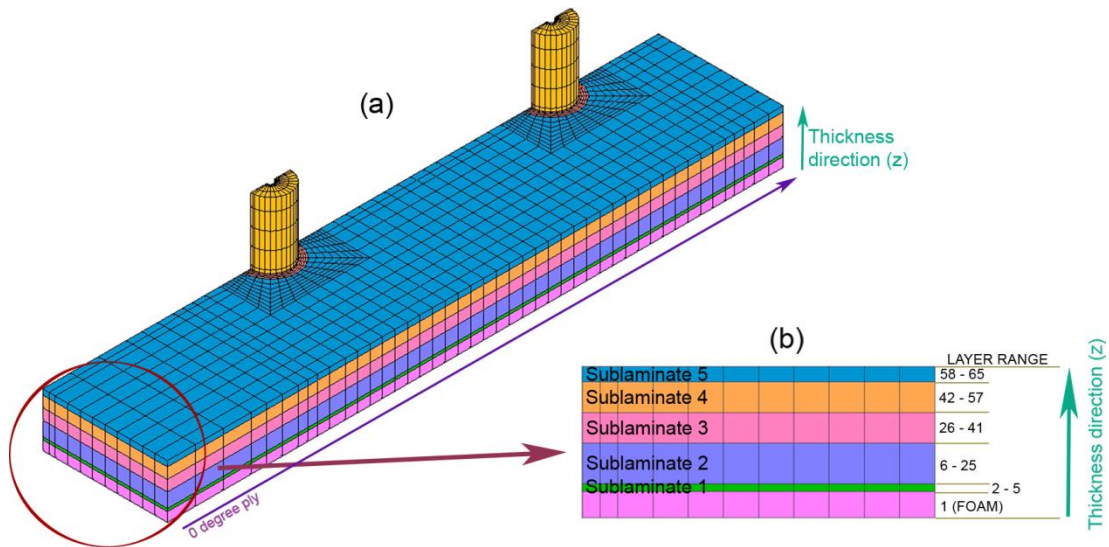
Figure 4.6 Sub-laminates and layer numbering.

4.2.2.1.1. Composite Brick Element (Element Type 149) [53]

One of the persistent difficulties in the analysis of composites is the unavailability of elements that are capable of multi-layered material modeling. The difficulty is compounded many times over by enhanced elemental output requirements that are necessary for making inferences. Unfortunately, the number of alternatives for layered material modeling is not even close to the diversity of non-layered element types. It is apparent that it is highly probable not to find an expected layered element type that is suitable for material model, geometric property, loading and non-linearity in question. Thus, when modeling composites, one should pay much more attention on finding suitable -or at least adequate- element type than modeling any regular material.

MSC.Marc® provides a wide range of element types (206), yet; only small number of these is applicable to composite modeling. Moreover, majority of "composite-capable elements" are not specialized on composite modeling, the ability is integrated by special functions such as SHELLSECT and COMPOSITE. As a result; during modeling multi-layered materials with MSC.Marc®, one should be very familiar with these functions and their usage.
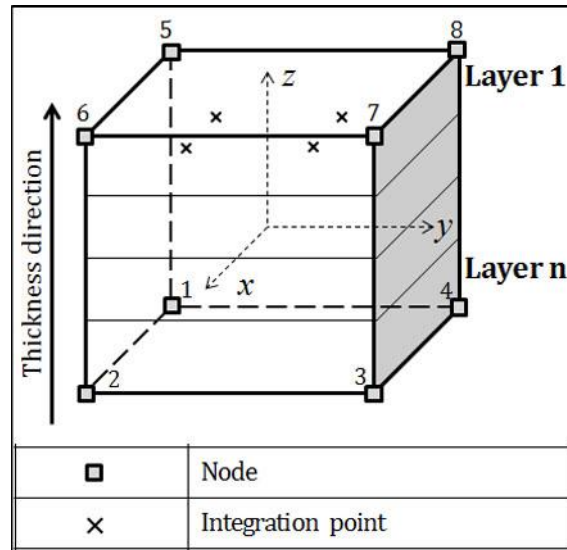
Figure 4.7 An illustrative figure of eight-node, 3D, composite brick element.

In this study, laminates are modeled as 3D bodies which makes COMPOSITE function is the only option for simulating the geometry. One benefit of this method is that, it brings the ability of solving various constitutive equations in single element, which enables evaluating various material behaviors through thickness. For instance; in a non-linear elastic-plastic analysis, a thickness section -or layer- might plastically flow whereas; another might still be in elastic region, and these behaviors can be tracked during post-processing. COMPOSITE function can be considered as a developed version of special shell element functions which modifies not only the number of integration points through thickness but also positions of the integration points, thicknesses of the layers and materials at these layers. As its name implies, it is mostly used for layered composite materials. These features of COMPOSITE function come from its ability of positioning integration points in the middle of each layer (Figure 4.7). Layers can have various thicknesses and they can hold different material properties. Additionally, COMPOSITE function changes through-thickness-integration method from *Simpson's Rule* to *Trapezoidal Rule*, which increases computational efficiency.

In the case of consideration, the most important geometric constraint is thickness, which brings in considerable transverse stresses that cannot be simulated accurately with shell assumption. Displacement field need to be calculated more precisely to calculate strains in thickness direction and this is possible with 3D models having more than one element through thickness direction. For 3D composite models, the most effective element type is 149. It is a three-dimensional, 8-node, continuum composite element containing different layers with different material properties. The element calculates all three direct stress and three shear stress components and regards coupling.

The element has 3 degrees of freedom and three coordinates. There are 4 integration points per layer. At each integration point, in-plane and interlaminar stresses and strains are computed. Element has a linear shape function. Integration is estimated using Gauss-quadrature method [53].

Element 149 is successful in estimating transverse normal stress, σ_{33} .However, for thick structures, transverse shear stresses cannot be accurately predicted for lamina level; in

analysis displacement is assumed to be continuous through-the-thickness; in real world cases, jumps in the displacement are seen along thickness. The derivatives of displacement with respect thickness direction are assumed to be also continuous; hence transverse shear strains are continuous. Calculating transverse stresses from these strains, a discontinuous stress between layers is obtained. In addition to this, since the element uses a linear function, transverse shear stresses do not disappear on the free surfaces of the part. Hence, for rational transverse shear results, geometry shall be divided along thickness [2, 54].

4.2.2.1.2. Brick Element (Element Type 7)

Type 7 is a three-dimensional, 8-node element. This element is used to model all the metal parts. Since strains are constant through the element, interpolation functions make it poor in shear calculations. But shear performance is improved by using assumed strain option.

4.2.2.2. Material Properties

In the analysis composite materials are assumed to be linearly elastic. For the steels, nonlinear properties are also defined. The details of the material properties are given in Section 4.1.2. .

4.2.2.3. Contact and Boundary Conditions

Contact conditions of the model are presented in Figure 4.4. Although introduction of contact brings in prominant non-linearity and difficulty; it is essential for this mechanism due to the complexity of the load path. MSC.Marc[®] has an efficient algorithm for contact analysis. It considers all the nodes belonging to exterior surface of a contact body as potential contact nodes that may touch a body; and all the outer surfaces (these are edges in 2D and faces in 3D) as potential contact segments that a node may contact. At every increment, positions of nodes are compared to check whether they are in contact or not. If they come in contact, appropriate links are constructed to avoid penetration of bodies and also to take into account the cases rise up due to the interaction of contacting surfaces like friction, heat transfer etc. [49]. Moreover; MSC.Mentat[®] is user friendly in contact definition, since user only defines bodies that are potentially in contact. There is no need of contact and gap elements. Additional contact parameters can also be defined if desired [49].

For the sake of efficiency model is reduced to quarter geometry by using symmetry surfaces x-z and y-z. These are frictionless surfaces and they restraint the displacement of the nodes that are in contact with these surfaces. These nodes will not separate from symmetry body. In constructed model; major contact bodies are bolts, laminate (lug), grip and bushings. Each of these bodies is in contact with symmetry surfaces. Their contact condition with respect to each other is shown in Figure 4.4.

Boundary conditions and force are presented in Figure 4.8. One side of the grip is constrained in all directions, whereas tensile is applied to the nodes located at the edge of the lug. Load is distributed through nodes by rigid beam elements (RBE2). Load is applied incrementally from 0 kN to 240 kN to ensure convergence and capture geometric and contact nonlinearity. Load increments are defined by the adaptive time step algorithm of MSC.Marc[®].
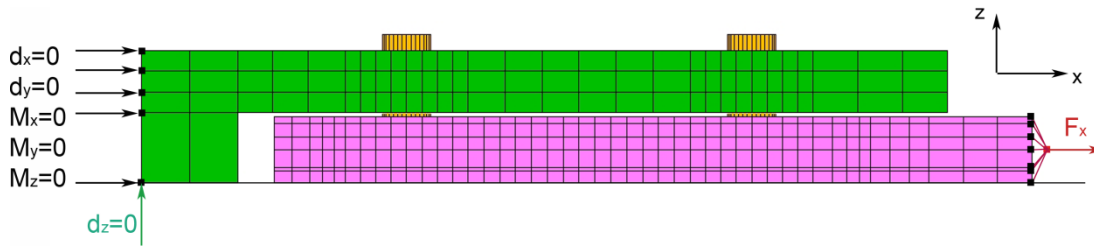
Figure 4.8 Loads and boundary conditions of the model.

4.2.3. Progressive Failure Analysis

As stated before, there are various methods to conduct a progressive failure analysis. Examples and specifications of studies on progressive failure analysis in literature are introduced in Section 2.3.1. Also a detailed comparison of the suggested procedures in literature and the procedure followed in this work is presented in the last section of the CHAPTER 2. This section is devoted to explanation of the method employed in scope of this work.

In this study, the progressive analysis method is applied using the finite element analysis tool Marc®.

The first step of a progressive failure analysis is the estimation of the strains and stresses and elasticity of the material is one of the factors affecting this calculation. In Marc® the property of the composite material is considered to be linear elastic until the onset of failure [49].

Next step of the progressive failure analysis is placing the strains or stresses in failure criterion for failure check. In literature there are numerous failure criteria; the Tsai-Wu, the maximum strain, the max stress, the Hashin and the Puck's are applied in the analyses of this study. A comparison of results obtained by implementation of each criterion will be presented later. The procedures and formulations of the criteria used are introduced in Section 3.3.

Failure criteria were developed to determine whether the composite can carry the applied loads exerted on it safely or not. The quantitative indicator for this is the failure index. Failure index (FI) evaluated by each criteria and the composite is said to fail when FI becomes larger than 1. The main function of progressive failure algorithm is activated at this stage of the analysis if failure is obtained.

When failure is detected, the related property with the failure is diminished according to the selected degradation rules. Different degradation procedures are the final cause of the dissimilarity of the results of various progressive failure analysis methods. The selective gradual degradation method is chosen in this study. Using this method, when failure indices become larger than one, a reduction factor depending on the value of failure index is assessed and added to the reduction factor of the previous estimation [49].

$$\Delta r_i = -(1 - e^{1-FI}) \tag{4.3}$$

For every failure index, this factor is calculated and used to diminish the related moduli and Poisson's ratios. For Poisson's ratios, the same reduction factors are utilized as the corresponding shear moduli [49].

$$E_{11}^{new} = r_1 E_{11}^{original} \qquad\qquad E_{22}^{new} = r_2 E_{22}^{original} \qquad\qquad E_{33}^{new} = r_3 E_{33}^{original}$$
$$G_{12}^{new} = r_4 G_{12}^{original} \qquad\qquad G_{23}^{new} = r_5 G_{23}^{original} \qquad\qquad G_{13}^{new} = r_6 G_{13}^{original} \qquad (4.4)$$

In progressive failure modeling, it is essential that diminished stiffnesses not be recovered in the following steps of the analysis.

After degradation of the material properties, the load of the current step is analyzed again to check whether extra failures are obtained after reduction or not. If there is no failure, the analysis resumes with the next step increment. If failure is obtained, the degradation procedure is reapplied.

Actually, progressive failure analysis utilizing the implicit finite element analysis tools is a bit problematic. Progressive failure requires degradation in the properties of the failed elements and the reduced stiffness of the structure (softening) causes difficulty in the convergence to equilibrium conditions. To obtain convergence, the codes require excessively small load increments which results in very long run times. What is worse, even for small load increments there is still a possibility of not achieving successful completion of the analysis.

4.3. Experimental Procedure

The structure described in Section 4.1. was tested in order to verify analyses results. Load and stroke data and strain data at defined locations were recorded during the test.

4.3.1. Test Set-Up

Tension tests of this study were performed in the laboratory of METU Mechanical Engineering Department. The machine utilized for tests is a Dartec, Figure 4.9, having a maximum loading capacity of 600 kN. The gripping of the specimen is done mechanically.

The machine is connected to its controller unit and data acquisition system.

The data acquisition system used for the tests is suitable only for measuring voltage output of the sensors that is not changing fast with respect to time (like in static tests). It has 8 channels and maximum data gathering rate is 8 data per second. The voltage measurements transferred to computer can be plotted and saved in real time with the help of the software the supplier of the system provided [55].

Figure 4.9 Test set-up.

4.3.2. Description of tests

Four different tests were conducted. The details for all are given in the following sections, however only Test D is investigated in detail in the scope of this study. Tests are named according to the sequential order they were carried out.

4.3.2.1. Test A

Test A is tension test of the composite laminate and the aluminum parts under design loads. In this test, the part named as adaptor-1 in Figure 4.1 is changed by a grip made of aluminum. Parts of this test are depicted in Figure 4.10 before and after mounting. Only one specimen is tested in this configuration and this assembly was also used in tests B and C.

The aim of this test was actually to prove both the aluminum parts and composite laminate resist design loads, which is specified as 60 kN.

4.3.2.2. Test B

Test B is fatigue test of the assembly described in Test A.

The aim is to prove the aluminum parts and composite laminate can sustain the loading fluctuating between 3 kN (tension) and 60 kN (tension) for 6000 cycles.

4.3.2.3. Test C

Test C is tension test of the assembly described in Test A.

The aim is to find the ultimate load carrying capacity of the structure. Hence, tension load is applied until failure.

Figure 4.10 Parts of tests A, B and C, before and after assembling.

4.3.2.4. Test D

Test D is tension test of the assembly displayed in Figure 4.10. This is the main test investigated in scope of this study. The aim is to find ultimate load carrying capacity of the composite laminate; hence tension load was applied until failure occurs.

A photograph of the structure before the test is shown in Figure 4.11.
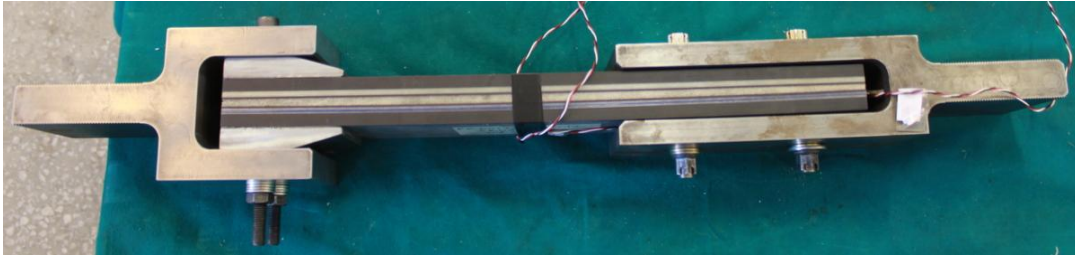
Figure 4.11 Structure tested in test D.

Test is performed controlling the displacement, with a speed of 0.015 mm/min. The load is applied until the ultimate failure is reached.

4.3.3. Instrumentation

The specimen previously described in Section 4.1. is instrumented with linear, 350-ohm strain gages with a gage length of 3.18 mm. The grids of the gage are made from constantan that is encapsulated within polyimide. This kind of strain gage is suitable for a static test. The reason for choosing a gage resistance of 350 ohm instead of 120 ohm is that heat generation rate is lower for higher resistances. Heat dissipation of composites are rather poor, hence this fact becomes important.

The gages are installed to the locations shown in the following figure. The representation SG 103,108 designates two strain gages that are applied on both sides (one on the front and one on the backside) of the specimen. The strain gages are connected to the data acquisition system with bridge completion cables. Utilizing these cables is a practical way of constructing a quarter-bridge configuration.
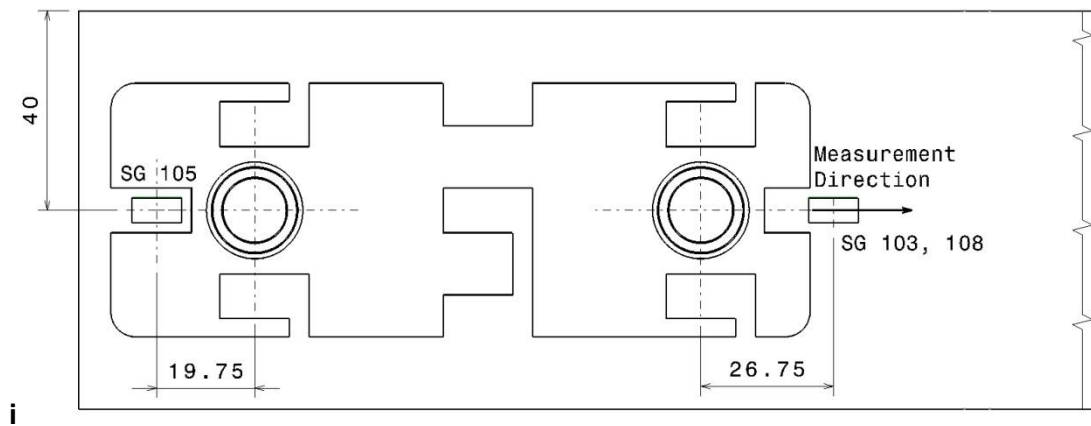
Figure 4.12 Locations of strain gages installed.

4.3.4. Data Collected

Data collected in the tests would be compared with the numerical analysis results.

As previously stated, data acquisition system has 8 channels. 1st channel collected data from load cell and 2nd channel collected data from LVDT, strains are read from the remaining 6 channels.

4.3.4.1. Processing Collected Data

All channels have their own filtering and amplifying circuit and hence gain constant. Gain constants found in the calibration of the system for an input voltage of 5.0007 V are given in the following table.

Table 4.7 Gain constants of channels

	Channels							
	1	2	3	4	5	6	7	8
Gain constants	397.5	396.9	397	397	397.3	397.4	396.9	397.3

Voltage output from data acquisition system has to be processed to transform to a more meaningful form. Conversion for the load and stroke data is done at the same time as the data is collected by the computer, since the formulation for them was defined previously. For the strain data, the output voltage is converted to strain using the formula:

$$V_o = \frac{-GF \times \varepsilon}{4} \times \left(\frac{1}{1 + \left(\frac{GF \times \varepsilon}{4} \right)} \right) \times V_i \times Gain \qquad (4.5)$$

Neglecting the term in parentheses, since it is very close to 1,

$$\varepsilon = \frac{-4V_o}{GF \times V_i \times Gain} \qquad (4.6)$$

CHAPTER 5

RESULTS and DISCUSSION

5.1. Numerical Analysis Results

Results of the finite element analyses are presented in this section.

In the following table the naming of the models are depicted together with a short description of which the model they represent, a more detailed explanations of the models are introduced in Section 4.2. . Explanations of the figures and legends of the graphs given throughout this study reference these designations.

In addition to the designations of the models, note that in some explanations within the text, the names of the criterion are used in abbreviated form, i.e. instead of "the Tsai-Wu failure criterion" only "Tsai-Wu" is utilized.

Table 5.1 Designations of models referenced in figures and graphs.

Naming	Description of Model	Maximum Load Solved
NPFA	Failure analysis without progressive failure method	240 kN
PFA-Tsai	Failure analysis with progressive failure method utilizing the Tsai-Wu failure criterion	205 kN
PFA-MaxStrain	Failure analysis with progressive failure method utilizing the maximum strain failure criterion	218 kN
PFA-MaxStress	Failure analysis with progressive failure method utilizing the maximum stress failure criterion	444 kN
PFA-Hashin	Failure analysis with progressive failure method utilizing the Hashin failure criterion	267 kN
PFA-Puck	Failure analysis with progressive failure method utilizing the Puck failure criterion	300 kN

The last column of the Table 5.1 shows the maximum loading can be solved for the model called out and a variation in these loads is obtained. Model NPFA, is all given a maximum loading of 240 kN and achieve this loading without any problems. However, a very high loading is applied to PFA models to obtain the load limit can be reached by the method applied. As can be seen in the table, not all the analyses succeed in solving the same load. The reason for this is the reduction of mechanical properties in progressive failure analysis. After a certain loading, stiffness and Poisson's ratio of the structure is reduced so that the model cannot be loaded stably any further. The analysis exits with an error message saying that the load increase at that increment should be smaller for continuation of the analysis. However, even a very low load raise is applied; the analysis cannot pass that step probably due to excessive reduction of properties. Since every failure criteria has different methods to evaluate failure indices, the properties that are diminished utilizing diverse criteria and the remaining stiffness of the model are also different. Hence, every model stops at different loads.

5.1.1. Elongation in loading direction

Elongation results in *x*-direction yields valuable information on failure progression. In the displacement vs. force graph, the change in the slope or sudden raise at a certain load indicates variation of stiffness of the structure. Hence, at these alteration points it can be concluded that some failure indices become larger than 1 (one) and the properties are diminished.

The elongation of the structure vs. force graph for progressive failure analyses with various failure criteria is presented in Figure 5.1. The descriptions of the abbreviations used in the following graph and in the text are given in Table 5.1.

The chart shows that:

- Until 12 kN the force increases in a linear manner for all models. Beyond this force, there is a slight decrease in slope of the curves. This diminution is seen just after the first load step. Hence, it can be caused by the closure of the initial gaps between the bodies as the load is applied. Another source of this kind of behavior can be the geometric and boundary condition nonlinearities that are induced by contact conditions.

- The linear like behavior of the elongation-force curve prevails until 168 kN.

- Near 150 kN, the slope of the curve slightly changed for PFA-Hashin and PFA-Puck criteria, but linear-like manner of the curve does not change.

- At about 168 kN, for the model PFA-Tsai the slope of the curve increased noticeably; and the slope of PFA-MaxStrain rise slightly.

- After 180 kN the change in the slope of PFA-MaxStrain becomes apparent and from 216 kN to until last step solved, there is a sharp increase.

- After about 200 kN, sudden rise of the elongation for PFA-Tsai is observed.

- The elongation-force curve of progressive failure analysis with the maximum stress failure criterion, PFA-MaxStress, follows almost draw the same curve with the model without progressive failure, NPFA. What is more, the end displacements of these two models are almost the same.

According to these facts, it can be deduced that except for PFA-Tsai and PFA-MaxStrain cases, no noticeable property degradation is exhibited for this load range. Nevertheless, this does not mean that no elements of these models experience any property reduction. Properties of some elements may be diminished, but the effect may remain local, so that it is not possible to catch these effects on the graph. From the graph, it can also be concluded that scarcely no property degradation take place for the model PFA-MaxStress or the diminution can only be effective in a very local region and cannot influence global stiffness of the structure; whereas PFA-Tsai is the case that is affected the most by the reduction. For PFA-Hashin and PFA-Puck analyses, stiffness reduction that can affect the global stiffness seems to happen at about 150 kN but this degradation is not dramatic so that the analyses can continue without creating unacceptable deformations due to extensive failure.
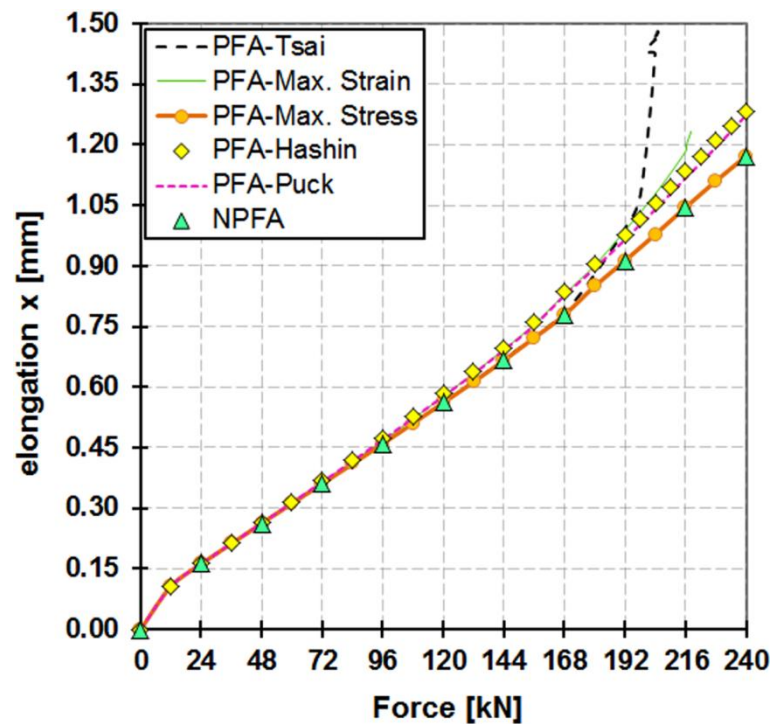
Figure 5.1 Elongation in x-direction vs. force graph of NPFA and PFA models

For PFA-Tsai from about 170 kN until 200 kN degradation is remarkable and after that, the decrease in stiffness is severe. Hence, the displacement increased suddenly. The limit of loading for this case is reached about 205 kN. After this load the analysis cannot continue even the load is increased at very small increments.

For PFA-MaxStrain, the reduction of the properties of structure is apparent after about 180 kN. A steep increase in displacements occurs just before the end of the analysis.

Hence, in the progressive failure analyses, examining the elongations in the loading direction gives an opinion on the failure status. When the properties are degraded, the elongation of the structure will be easier, and hence the slope of the elongation-force curve will increase. Steep increases of elongation in the graph illustrate an important reduction in stiffness of the structure. Investigating elongation-force curves of the analyses, PFA-Tsai is specified as the model experiencing the maximum degradations at the maximum load that the analysis can solve. Second critical case in terms of property diminishment is observed for PFA-MaxStrain. On the contrary, almost no property diminution occurs in PFA-MaxStress. For the remaining cases, PFA-Hashin and PFA-Puck criteria, property degradations are present; but these do not cause a very large impact on the global stiffness of the structure. Considering all these, the Tsai-Wu failure criterion is obtained as the most conservative failure criterion for the analysis of this structure. At a load level that other criteria almost show no failure, the analysis with Tsai-Wu failure criterion had to stop due to excessive deformations, and hence property reductions take place. On the other hand, at the same loading conditions estimations with the maximum stress criterion shows large margins to significant failures.

The effect of property degradation can be detected also by visualizing the deformed shape since the reduced stiffness elements will experience larger deformations. Deformed shapes of the analyzed structure for the models NPFA and PFA-Tsai, both loaded to a 205 kN tensile force, are exhibited below. The global distortion of the structure is almost the same for all the analysis cases, whether progressive failure or not, as can be seen in (a) and (b) of Figure 5.2. However, the effect of progressive failure analysis is obvious inspecting detailed views. In detail C almost no deterioration is seen in the composite structure. On the other hand, the shapes of the elements around the hole altered significantly for the progressive failure analysis case shown in detail D. This proves the degradation of the properties of these elements.
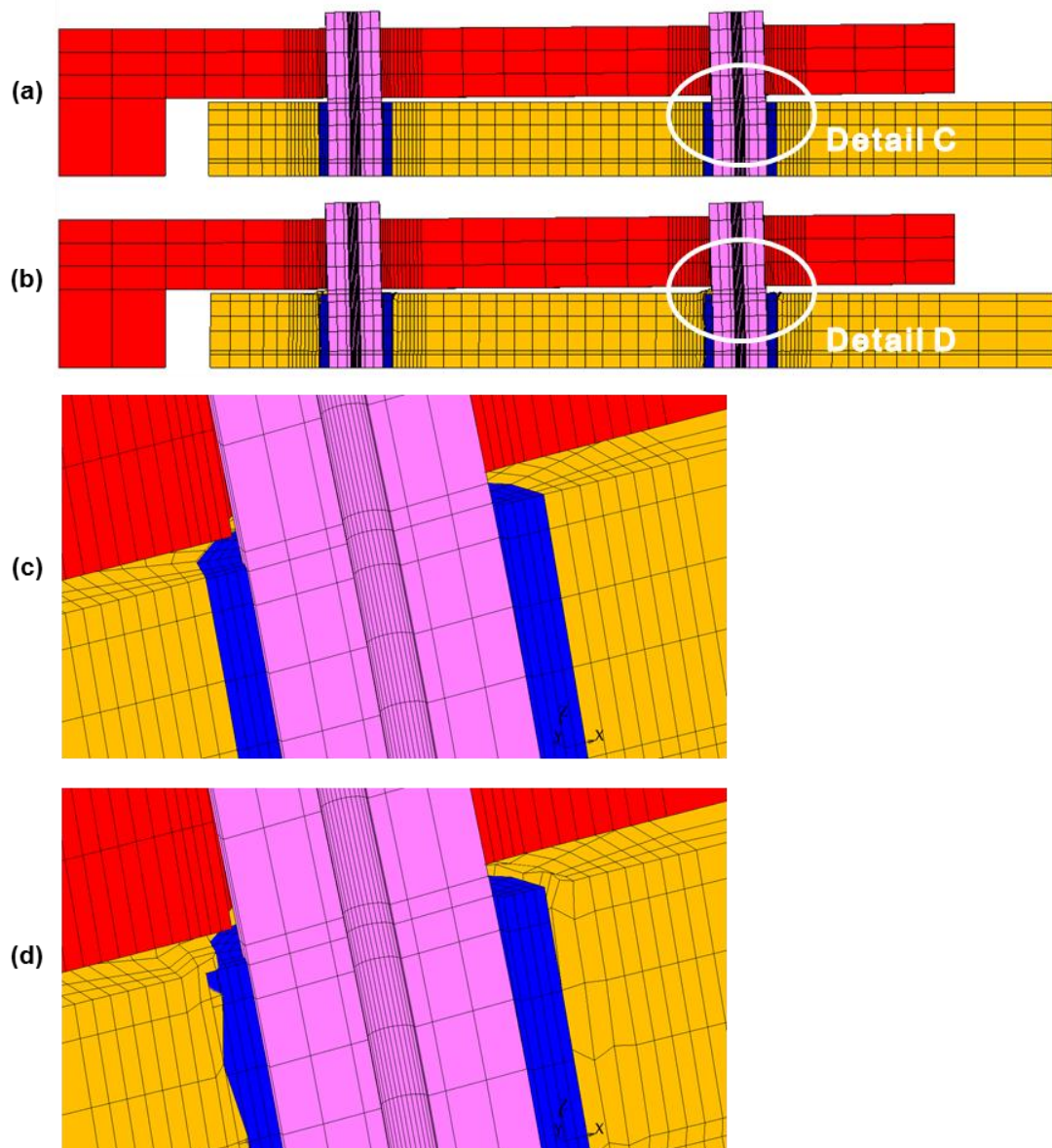
Figure 5.2 Deformed shapes at about 205 kN tension (a) model NPFA (b) model PFA-Tsai (c) detail C (d) detail D

5.1.2. Failure Prediction

The load at which failure initiates, the mode of failure and the ultimate loading that a structure can withstand are in scope of failure analysis. In this study the failure predictions of various failure criteria with and without progressive failure analysis is evaluated. In order to visualize all the predictions of the analyses, failure index plots of different failure criteria which are obtained from the analyses without progressive failure and damage plots of different failure criteria obtained from the analyses with progressive failure are presented.

5.1.2.1. Failure Prediction without Progressive Failure

In this part, failure indices obtained by analyses performed without implementation of progressive failure method are introduced.

The following figures show failure index contours of some layers of the structure. Failure indices of the structure changes at each layer; however, it is neither practical nor necessary to display plots for each layer within this thesis report. Instead, results of each layer are evaluated previously and a set of layers that will exemplify the failure of the structure are chosen, plots for them are presented flowingly.

For the selection of plies of which results are depicted, the idea is to pick one lamina from each group of lay-ups. As mentioned earlier in Section 4.2.2.1. , in the construction of the model, the laminae are grouped according to their lay-ups and materials to form sub-laminates. Within these groups, group 1 and 5 show similar characteristics, the same situation is also true for groups 2 and 3. Hence, choosing only one ply from either group 1 or 5, which one is more critical; and only one ply from either group 2 or 3 is enough. Foam structure is out-of-scope in terms of failure results, since it is assumed as isotropic. Hence, merely 3 layers are enough to demonstrate the failure of the structure.

For ply selection, examination of how critical the layers is made considering the failure indices of Tsai-Wu criterion solution. Layers 25, 43 and 58 are found to have the most severe damages among the sub-laminates they represent. The plots for failure prediction are given for these layers hereinafter. Please refer to Figure 4.6 for positions of the layers within the laminate.

Failure index contours of the chosen plies obtained with different criteria for three loading conditions are represented in the figures. The maximum strain, the maximum stress, the Hashin and the Puck failure criteria yield more than one failure index. The explanations of these indices are introduced in Section 3.3. For the failure criteria having more than one failure index, the index to be presented is also selected. Two things are taken into account making this choice: how critical the failure mode and comparability with another criterion. For instance, for layer 25, in-plane shear failure indices are plotted for maximum strain and maximum stress failure criteria. For this, initially the failure indices of these two criteria are decided as comparable (similarly Hashin is chosen to be comparable with Puck); hence, the same failure index is to be plotted for these. Then, the failure index values are controlled and results of maximum strain is identified to be more critical. Finally, the failure mode yielding the highest index is searched for. And the outcome of the maximum stress criterion is to be shown as compatible with this selection, even though for maximum stress another index is more critical. For instance for the layer 25, the highest and most widespread failure indices are obtained at in-plane transverse direction, however the results are presented for in-plane shear to be comparable to results of maximum strain.

In these figures, elements having failure index greater than 1 is expected to be failed. Investigating figures of all the layers displayed, the largest deteriorated areas occur for the maximum strain criterion. The layers seem to be almost completely failed at 240 kN for this criterion, while the number of failed elements obtained by other criteria is much less. Thus, it is concluded that the maximum strain criterion gives the most conservative results. However, it cannot be deduced that the maximum strain criterion is the most conservative method among all. Maximum strain is the only method investigated in this study that is not stress-based, using strain allowables to check failure. Actually there is no test data available for strain allowables thus, for almost all allowables of strain, assumptions are made to estimate a value that can be used as a strain allowable. Making such assumptions may be a cause of extensive failure of layers analyzed with maximum strain criterion. On the contrary, stress allowable data attained by tests exists for the glass and carbon composite materials used, except for out-of-plane properties. Due to all above-mentioned situations, results obtained

with stress-based criteria of this study may show more realistic result than the results with strain-based criteria.

A problem in failure indices due to unreliable material properties may also be present for Hashin and Puck failure criteria. These criteria requires the allowables of matrix and fiber materials both for tensile and compression loading conditions. However, the mechanical property data available is only for in-plane strengths of lamina. Therefore, fiber and matrix strength values are assumed. Furthermore, fracture envelope slopes used in the Puck criterion are also assumed values.

For all the layers, NPFA-Tsai-Wu show large areas where failure indices are smaller than zero. Negative failure indices do not describe any physical situation.

Hashin and Puck criteria yields similar results for all the layers displayed. For both Hashin and Puck criteria the displayed failure mode is for matrix. This means that for those layers and load cases failure indices of matrix material show a more critical status compared to the case of fiber. This is an expected result since the structural failure is typically starts in the matrix. When the failure index points to a critical case also for fiber, this is usually a sign of complete failure of the structure. The plots given in Figures 5.3 to 5.5 represent that the failure is initiated in the matrix in the compression sides of the holes.

Assessment of the failure index plots that display the analyses results without progressive failure shows that for all the critical plies, the maximum strain criterion yields the largest failure area. If reliable material data existed for strain allowables, this criterion will certainly be specified as the most conservative criterion among all. However, since these properties are assumed values, it can only be deduced that under these circumstances, the most conservative case is represented by the maximum strain criterion. For also failure index plot evaluation, the maximum stress criterion exhibits an intact structure.
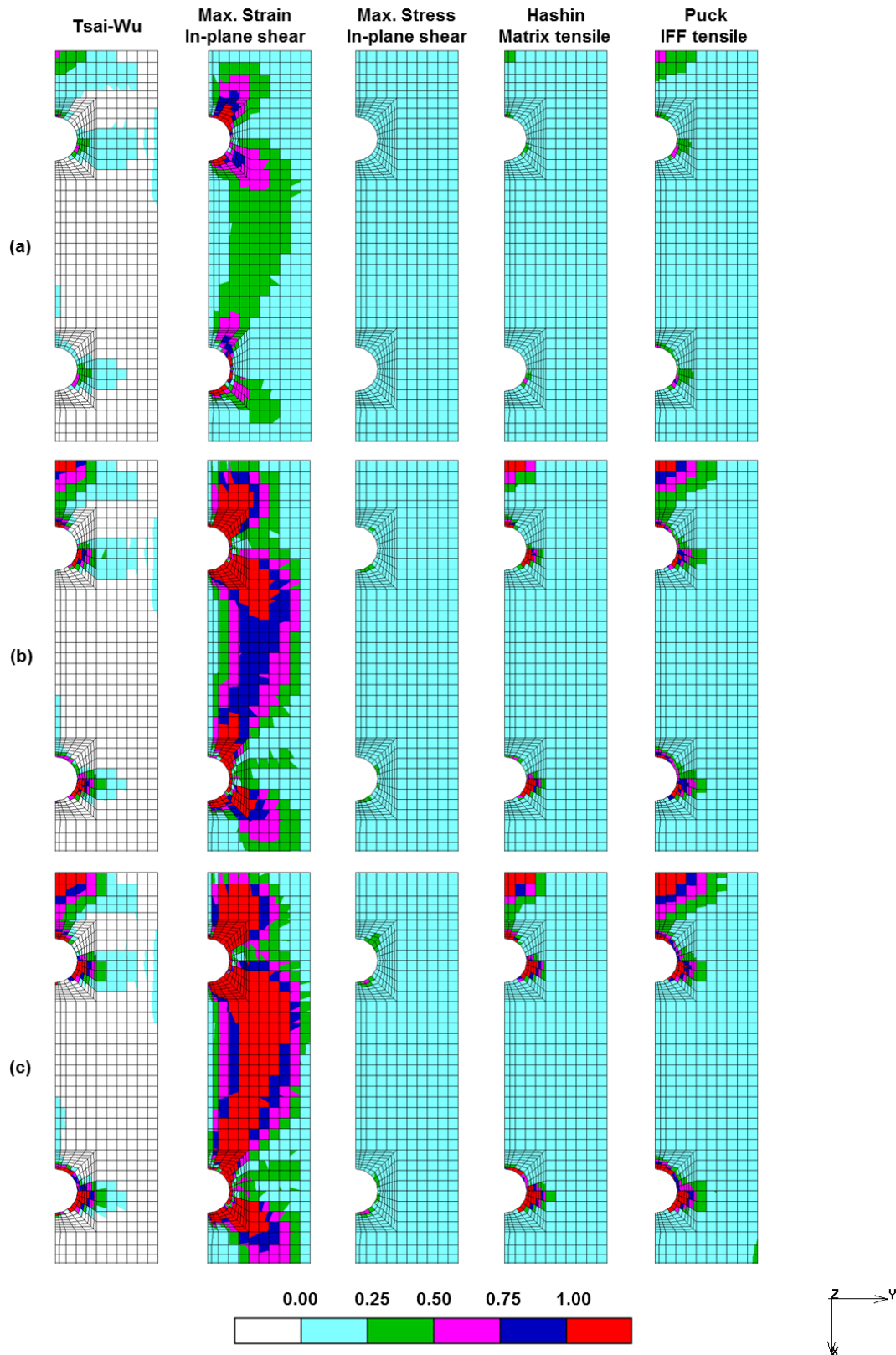
Figure 5.3 Failure index plots for layer 25 (glass UD 0º) at (a) 72 kN (b) 168 kN (c) 240 kN.

50
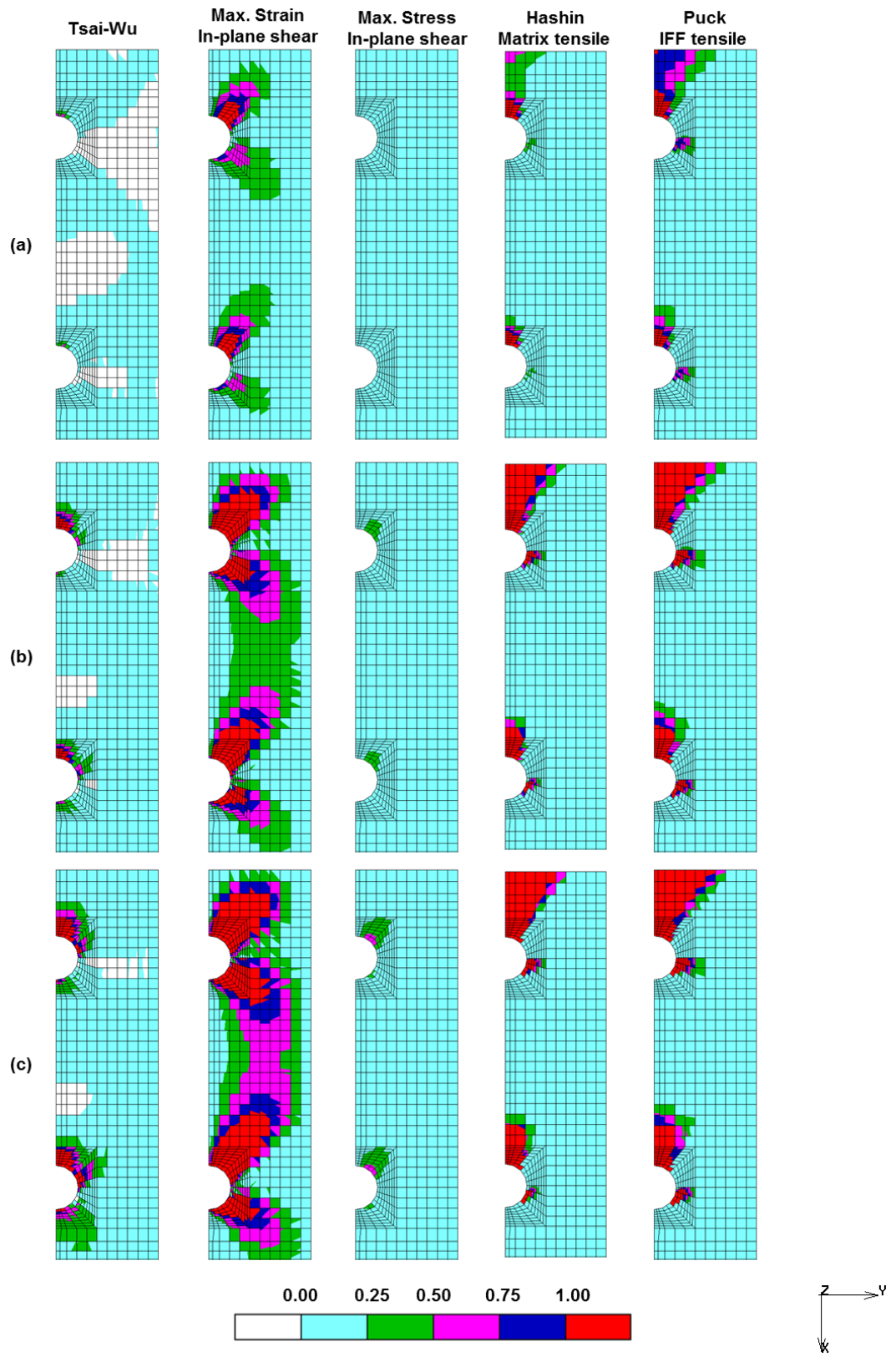
Figure 5.4 Failure index plots for layer 43 (carbon fabric 0º) at (a) 72 kN (b) 168 kN (c) 240 kN.
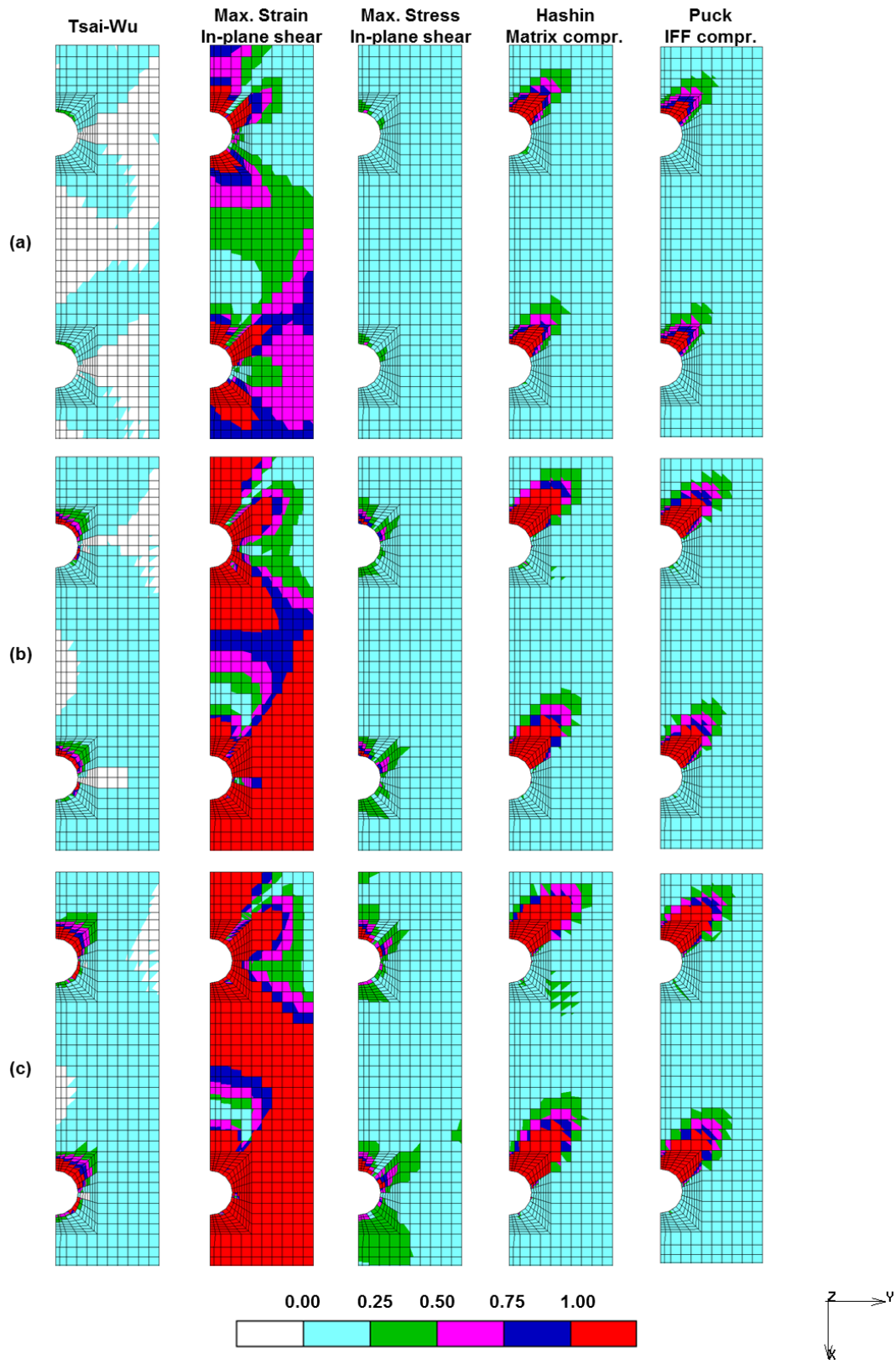
Figure 5.5 Failure index plots for layer 58 (carbon fabric 45º) at (a) 72 kN (b) 168 kN (c) 240 kN.

5.1.2.2. Failure Prediction with Progressive Failure

In this section, damage results obtained by progressive failure analyses are visualized utilizing the post-processor MSC.Mentat®.

Damage plots define the level of degradation of properties at a load step. For instance, 0.5 damage of an element means a stiffness reduction of 50%. The maximum damage can be read from the plot can be 0.99 since the employed residual stiffness factor is 0.01 for the analyses performed in this study. Residual stiffness factor defines the minimum value that the stiffness of the material can be reduced. Beyond this minimum, no more degradation is possible and full damage is said to be reached.

Another important property of the damage plot is that it displays the maximum damage evaluated, by ignoring the mode of failure. Hence, it is not possible to obtain whether fiber or matrix is failed from these plots. On the contrary, this information can be obtained from failure index plots of analyses without progressive failure. In a damage plot, for instance applying the Hashin failure criteria, if degradation of matrix is larger than degradation of fiber at an integration point, the damage data of the matrix is collected; then at the same loading for another integration point if degradation of fiber is higher, damage data of the matrix is collected this time. The plot is formed following this procedure [56].

Damage information within the structure changes at each layer, but plots for all of them are not given in this thesis report like for the case of failure index plots. The procedure followed in the choice of layers to be presented is explained in Section 5.1.2.1. In this section, damage plots of the previously selected layers 25, 43 and 58 are depicted.

In all the following figures below, a black box is drawn around the results of the Tsai-Wu and the maximum strain failure criteria at row (c) to attract attention. This implies the picture given does not actually belong to 240 kN load case. Analyses with both the Tsai-Wu and the maximum strain failure criteria are stopped before 240 kN is reached, and the results given in the figures shows the last load step can be solved. This is 205 kN for the PFA-Tsai and 218 kN for PFA-MaxStrain cases.

Examining the following figures, it is obvious that the maximum strain criterion case yields the largest damage areas for all the layers and loads displayed. Also without progressive failure, the extent of the areas that failure indices are higher than 1 is the largest for the maximum strain criterion as can be seen in Figures 5.3 to 5.5. Since progressive failure is activated when any of the failure index becomes larger than 1, there is a relation between these plots. Considering this, having the largest damage area for the maximum strain criterion was presumable. Damage basically follow the path of failure indices becoming higher than 1, however as the material properties are reduced during progressive failure analysis, the damaged area can spread more than the area of failure indices higher than 1.

For all the layers and all the criteria the failure initiates around the holes. For 0° plies, there is also a damage progression observed starting at the edge that is close to hole 1 of the structure.

As stated previously and presented in Figures 5.6 - 5.8, the maximum damage areas are exhibited by the maximum strain case, PFA-MaxStrain. This is followed by PFA-Tsai, PFA-Hashin and PFA-Puck. The maximum stress criterion nearly does not show any damage progression. Conversely, for maximum strain criterion nearly all the elements of the ply have completely failed at the last load step. Furthermore, the solution with the maximum strain criterion reaches that limit even though the last load step solved (218 kN) is lower than the forces applied in the analyses with other criteria (240 kN). A similar situation is also obtained for the PFA-Tsai. Actually, PFA-Tsai yields a more critical condition than PFA-MaxStrain, since at a lower load, 205 kN, the complete damage is observed without damage can spread widely.

For the PFA-Tsai analysis, after the complete failure of all the elements around the holes, the failure indices may become larger than one for a wide range of elements within the structure; so that the deformations may become so large that the analysis could not continue anymore and stopped suddenly. The reason why the PFA-Tsai shows such a behavior is tried to be explained studying the formulation of the Tsai-Wu failure criterion. First of all, Tsai-Wu failure criterion is a quadratic criterion. Thus, with this criterion the stresses always cause a more critical situation compared to linear criteria like the maximum strain and maximum stress criteria. Thus, Tsai-Wu criterion could be expected to predict more critical cases than these criteria. On the other hand, the Hashin and the Puck criteria also have quadratic stress terms. The results they predict do not present such a critical situation as for the Tsai-Wu though. The difference of these criteria from the Tsai-Wu criterion is that they differentiate between the failure modes. For every failure mode, the stress terms that can cause that failure mode is utilized. However, Tsai-Wu failure criterion integrates all the stress terms in a single formulation. These facts may be the results of the sudden complete damage of the structure at a lowest load for the PFA-Tsai analysis.
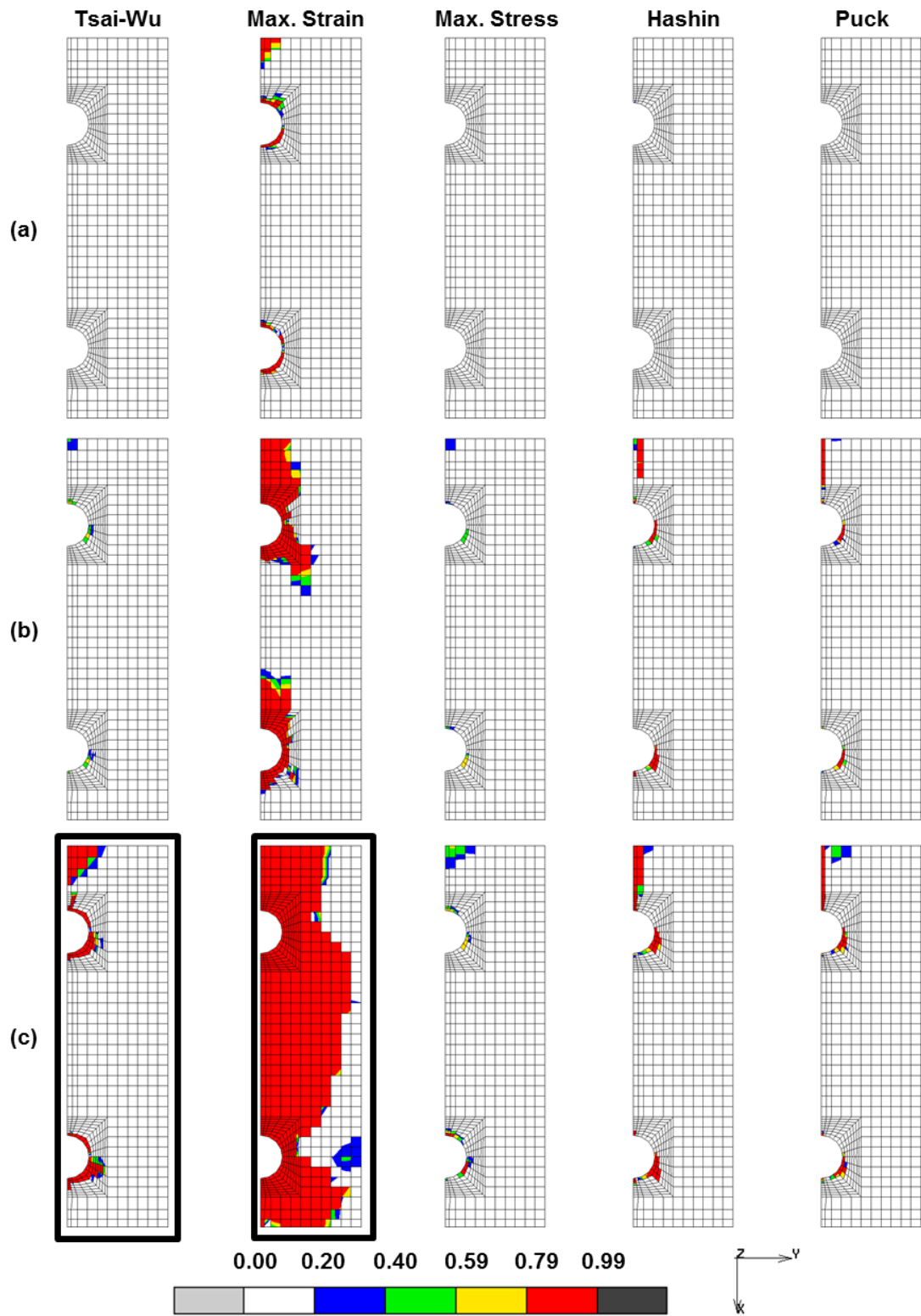
Figure 5.6 Damage plots for layer 25 (glass UD 0°) at (a) 72 kN (b) 168 kN (c) 240 kN
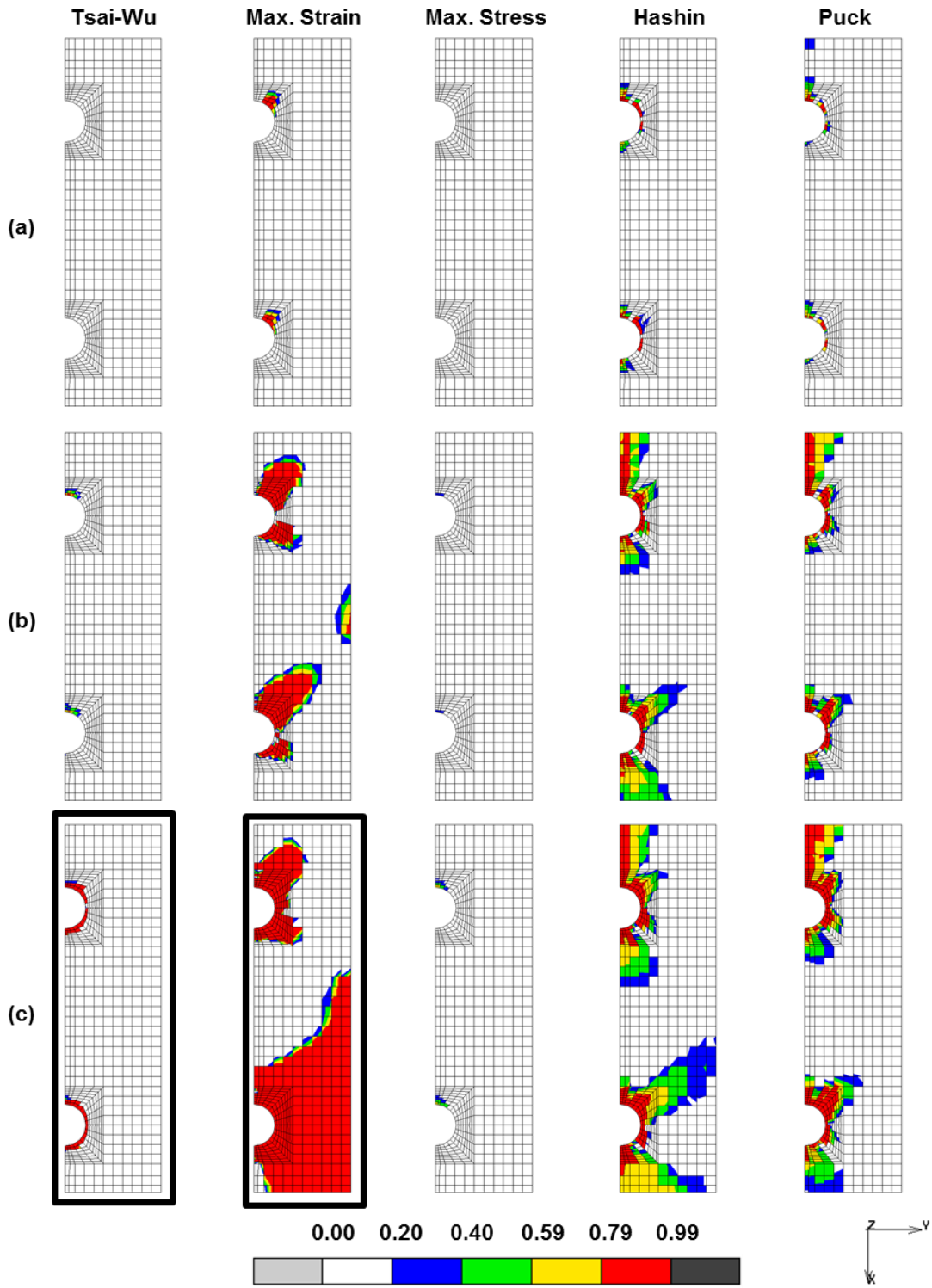
Figure 5.7 Damage plots for layer 43 (carbon fabric 0º) at (a) 72 kN (b) 168 kN (c) 240 kN
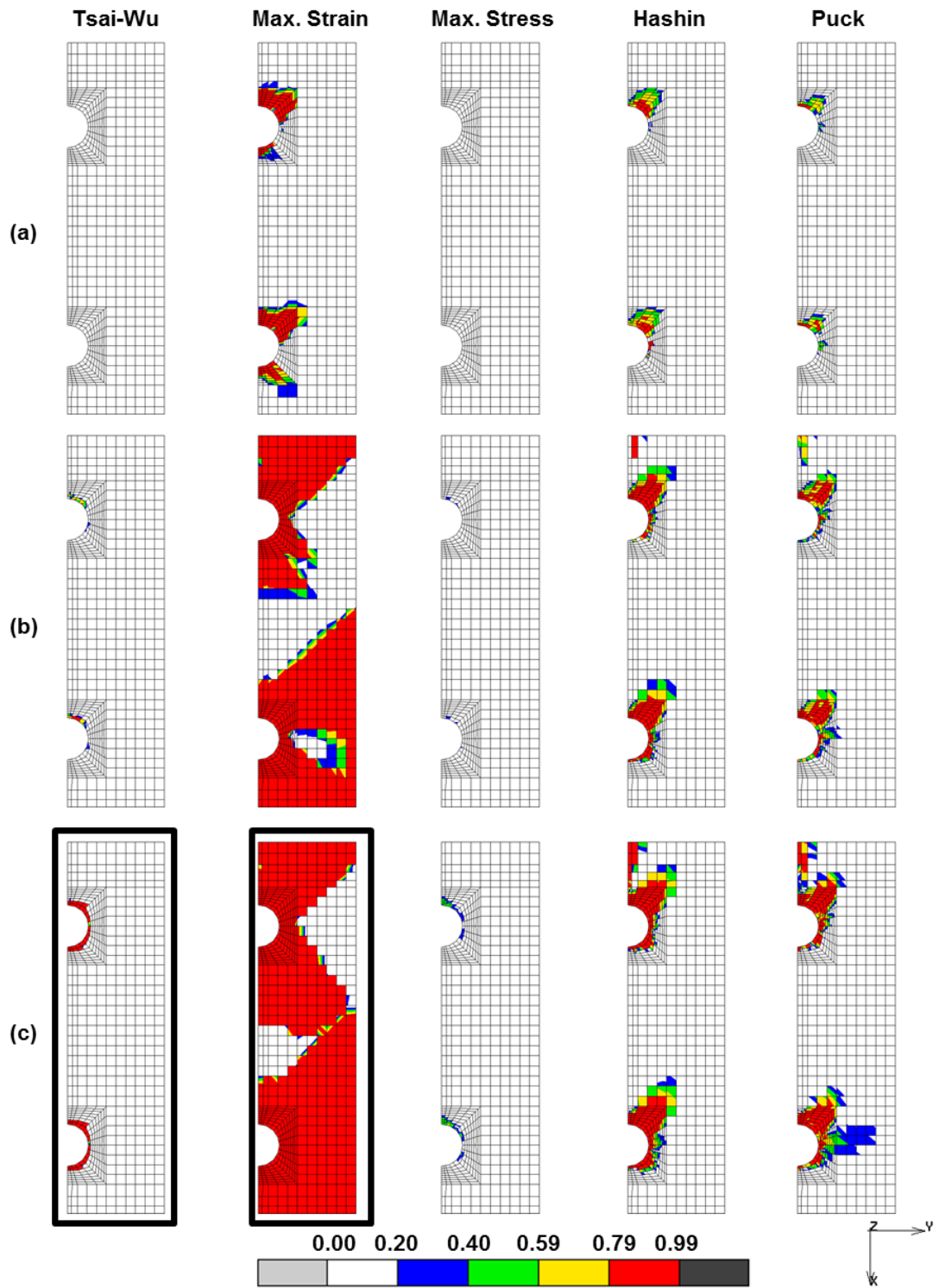
Figure 5.8 Damage plots for layer 58 (carbon fabric 45º) at (a) 72 kN (b) 168 kN (c) 240 kN

57

In Part 5.1.1. the deformed shapes of the damaged elements are given for the progressive failure analysis of the Tsai-Wu failure criterion. From the deformed shape, it was deduced that the stiffness of the elements around the hole is degraded. The previous damage plots affirm this conclusion since the elements around both holes are fully damaged for the case PFA-Tsai.

5.1.2.3. Comparison of Results with and without Progressive Failure Analysis

Comparison of results with and without progressive failure analyses are given in this section.

First ply failure loads obtained implementing different failure criteria are presented in the following table. These values point to the load at which the properties are started to be degraded for the progressive failure analysis. For design purposes, if substantiality of a structure is questioned without progressive failure, the laminate is assumed to be totally failed when first ply fails. However, composite laminates actually fail at larger loads than the estimated values with first ply failure approach. Progressive failure analysis is useful in that it shows what will happen if these first ply failure forces are exceeded. The designer can then decide when the failure within the laminate is actually gets critical and cause the laminate to fail. Hence, progressive failure analysis offers a way to get rid of over-safe predictions and designs.

Table 5.2 First ply failure load predictions of various criteria.

	First Ply Failure [kN]
Tsai-Wu Failure Criterion	60
Maximum Strain Criterion	12
Maximum Stress Criterion	84
Hashin Failure Criterion	24
Puck Failure Criterion	24

In the analyses in scope of this study, if the first ply failure is chosen as method for checking the failure of the laminate, the values presented in the above table will be presumed as the maximum forces that the laminate can withstand. However, the results of the test prove that these values are too conservative. In a progressive failure analysis, the stiffness of the failed plies is degraded and the forces are redistributed to adjacent plies. If the structure can still sustain the loading after this stiffness reduction, the analyses can continue with higher loads. This iteration enables determining a more realistic ultimate load carrying capacity demonstrating a better simulation of the actual failure mechanism of a composite laminate.
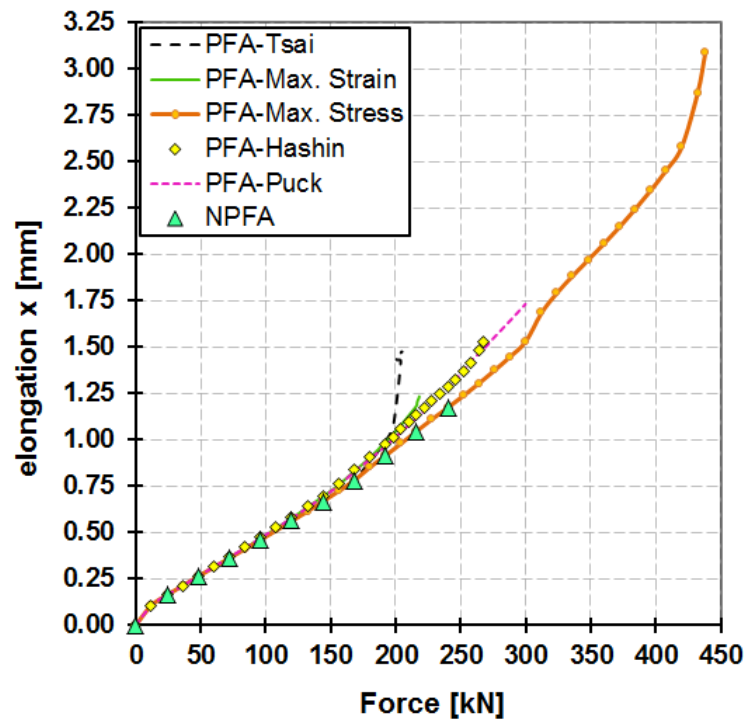
Figure 5.9 Maximum load predictions with various failure criteria.

Figure 5.9 shows the elongation vs. load curves that are obtained by progressive failure analyses applying various criteria. The end of each curve in the graph depicts the limit that the analyses can continue without any numerical problem and thus the maximum load prediction of these analyses for this structure. Examining all the results, it is observed that the progressive failure analysis with the maximum stress criterion yields the highest load prediction whereas progressive failure analysis with the Tsai-Wu criterion gives the lowest. Hence, it can be concluded that for the analyses of this structure Tsai-Wu is the most conservative criteria. Still, the ultimate load capacity of about 200 kN it provides is much more reasonable than the prediction of the first ply failure approach, which is 60 kN.

In Figure 5.10, the damage plots for the top layer (layer 65) are presented. From this plots, the extent of the damage on the top ply when the indicated loads are reached can be seen. If we define the damage behavior as a measure of damage tolerance, the maximum strain criterion will be the method that yields the most damage tolerant behavior, while the Tsai-Wu and the maximum stress criteria will be the least damage tolerant.

The results obtained with progressive failure analysis shows that the structure can carry more loads safely than the predicted values by the first ply failure load. The difference is as much as 12 times for some of the cases. However, the accuracy of the predictions of the loads that the progressive failure analysis yields shall also be carefully evaluated. The comparison of the analyses results with the test cases will be presented in the following sections.

59
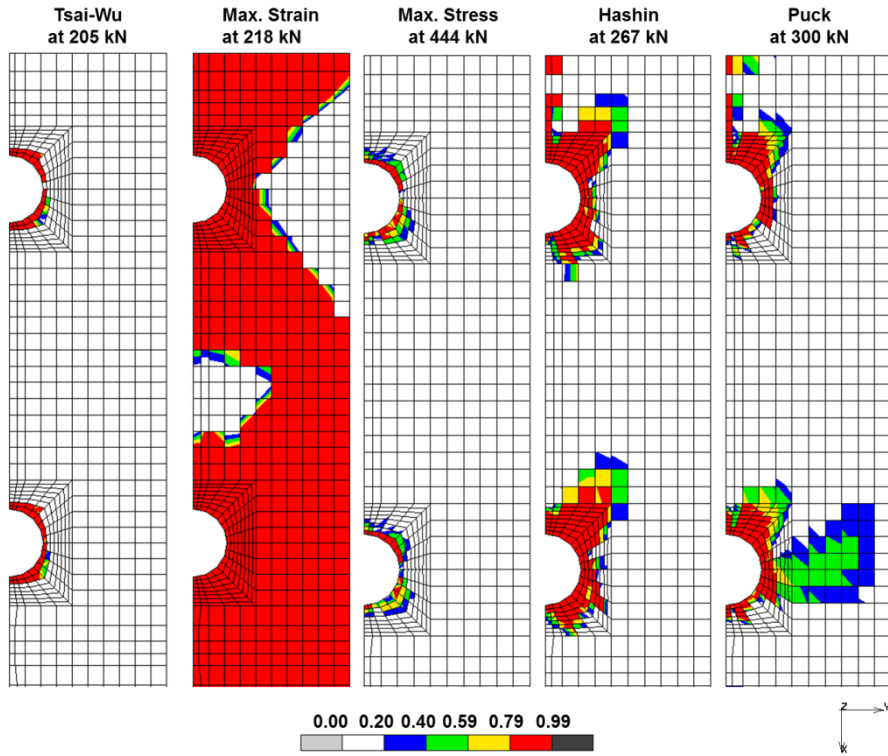
Figure 5.10 Damage plots of layer 65 at the specified loads.

5.2. Test Results

The results obtained in the test is given in this section. The data presented belongs to test D of which the details are previously presented in Section 4.3.2.4.

Figure 5.11 The specimen before the assembly and before the test.

A photograph of the specimen before the assembly and before the test is displayed in Figure 5.11. The photograph showing the assembly tested is given in Figure 4.11.

The maximum load obtained in test D is 240 kN at 608 s. The test is ended by the fracture of two bolts connecting the test assembly with the moving grip of the test machine. Because of the bending of the bolts before ultimate failure, the foam structure in the middle of the specimen is compressed and after unloading it is observed that the foam structure is separated into two. The photographs taken after the test is given in the following figure.
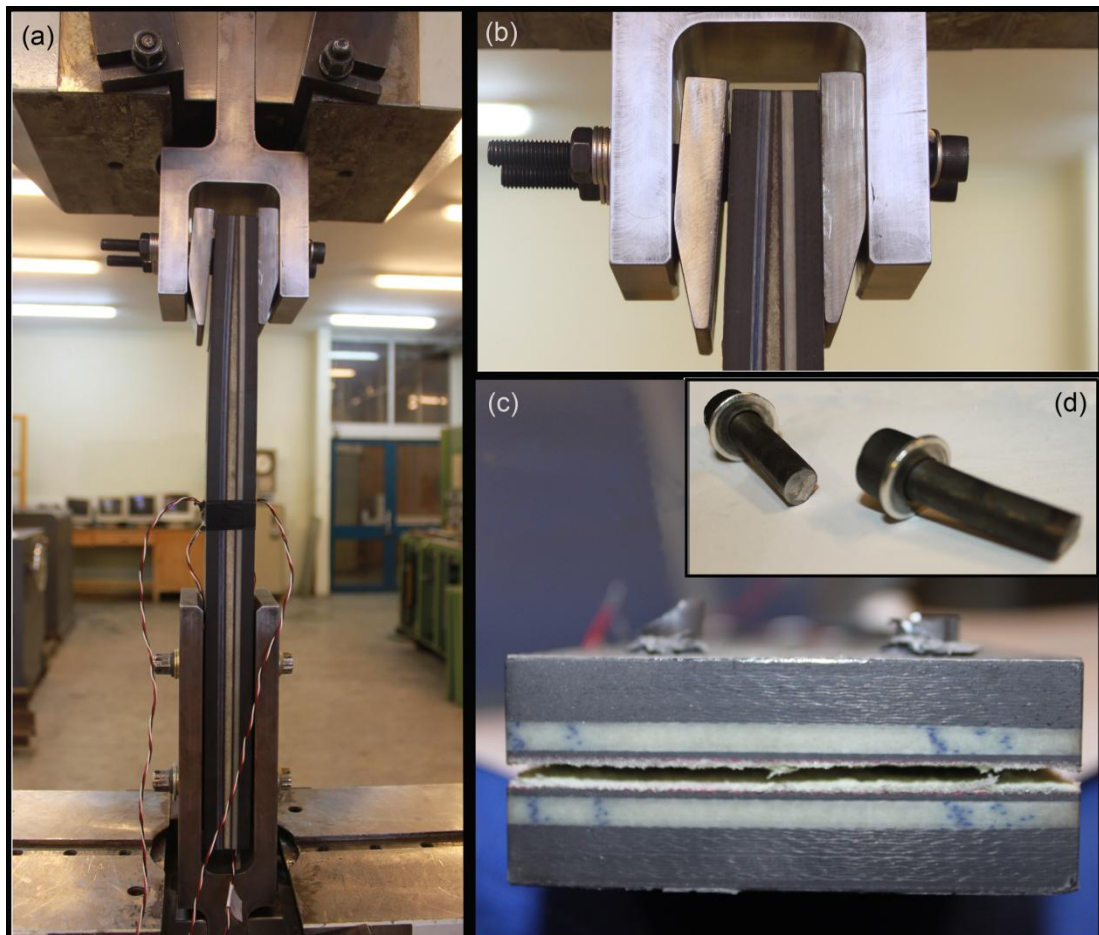
Figure 5.12 End of the test (a) View of the complete assembly (b) Failure of bolts and compressed foam structure (c) Separation of foam after unloading (d) Failed bolts.

The force versus stroke graph based on the data collected during tension test D is depicted in the following figure. The graph shows dominantly the characteristics of the bolt material.

The reason of having very large stroke readings may be due to the bending of the bolts during the test. In addition to this, the accuracy of the calibration of the machine and the data acquisition system are to be questioned, since there are no parts that can allow such large deformations without catastrophic failure.
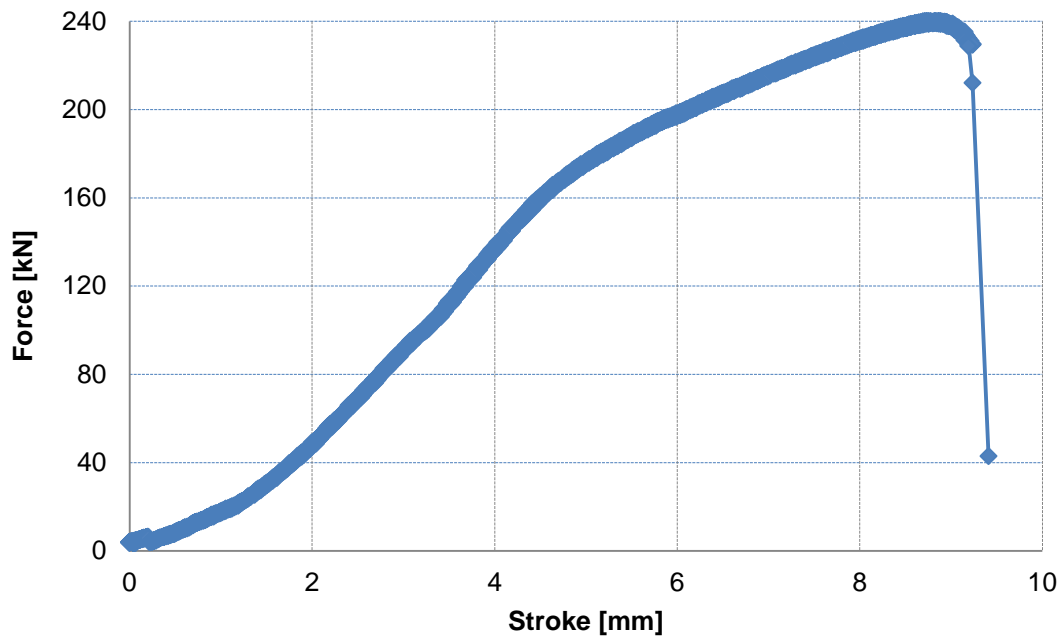
Figure 5.13 Force vs. stroke graph for tension test D.

5.3. Comparison of Numerical and Test Results

In this section, the correlation between the results obtained from finite element analyses and experiments are evaluated. The comparisons of strains and failures that can be seen with naked eye are made.

The strains obtained from the model without progressive failure analysis, "NPFA" and progressive failure analysis models each utilized different failure criteria "PFA's" (the explanation of the designations are given in Table 5.1) are compared with the strains collected during tension test D (refer to Section 4.3.2.4. for details of test D).

The failure index vs. load graphs displaying the load that the failure initiates and the strain vs. force graphs are presented in the following figures.
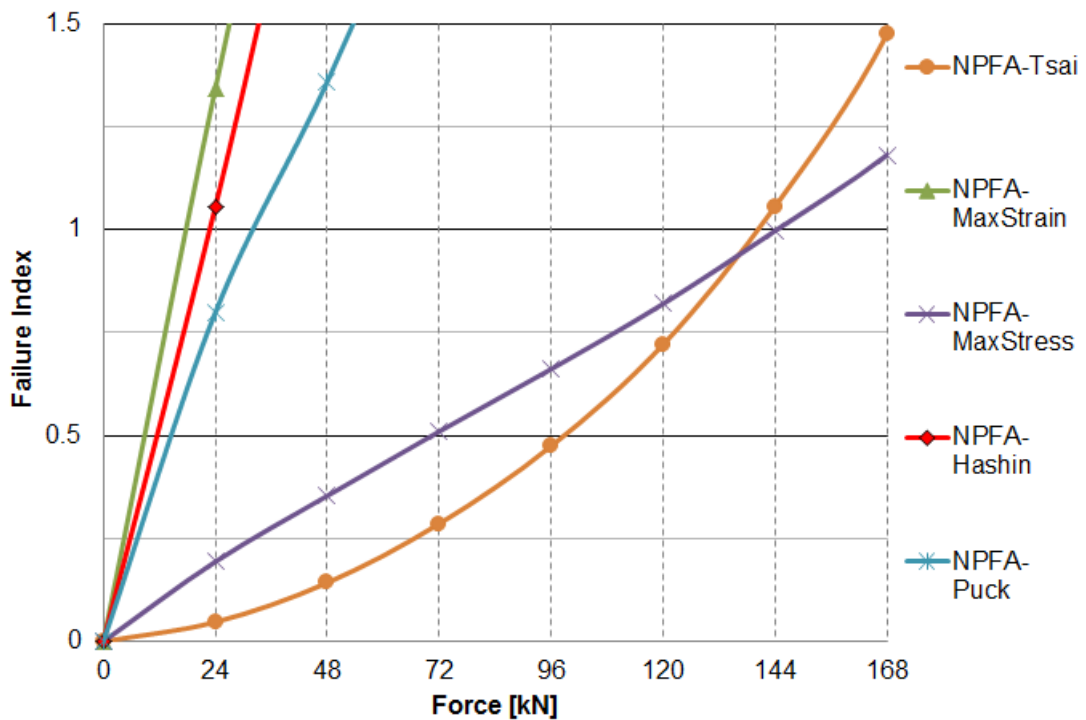
Figure 5.14 Failure index vs. load graph for layer 65.

The Figure 5.14 represents the loading that the failure indices with various failure criteria get higher than 1, which points to initiation of failure within a layer. These analyses are performed without progressive failure. The displayed failure indices are the highest attained values on the layer 65 at the specified tensile load. According to the graph, NPFA-MaxStrain and NPFA-Hashin criteria are the first criteria yielding failure. These are followed by NPFA-Puck, NPFA-Tsai and finally NPFA-MaxStress. The consequences of showing the first failure on a layer, on the last failure state of the structure are discussed in the following.

Investigating the Figure 5.15 for strain gage 103 location:

- The strain values increase in a linear manner except for PFA-Max Strain and PFA-Tsai cases.

- A good estimation of the trend of the strain-force curve is made. The slopes of strain-force curves obtained from the analyses are similar to the strain-force curve drawn with the data recorded in the test except PFA-Max Strain and PFA-Tsai.

- The strain data is calculated approximately with 5% error. The only problem may be that the assessed values under-predict the strains of the test. Still, the error is not high and the values are acceptable.

- For the progressive failure analysis with the Tsai-Wu and the maximum strain failure criteria, the discussions are made regarding also the elongation in x-direction vs. force curve given in

- Figure 5.1. These two curves do not necessarily give the same trend since the strain values show local whereas elongations show global effect of progressive failure. However, examining them together enables clarifying the effect of progressive failure analysis if changes in strain occur simultaneously with changes in elongations.

- For the case PFA-Tsai, the values draw almost the same curve as the results of other analyses until 168 kN. From that loading to 192 kN, the slope of strain-force curve shows a small increase. It is presumed that this slight deviation arises from the stiffness reduction due to failure in the composite structure since at the same load level there is also an increase in the elongation. After 192 kN, there is a decrease in strain, in other words the stiffness increases. This can be interpreted as a local phenomenon due to redistribution of strains owing to local failure of elements. Therefore, this should not be taken as global structural stiffening. Besides, the trend of curve in Figure 5.1 ensures the structure does not stiffen after 192 kN.
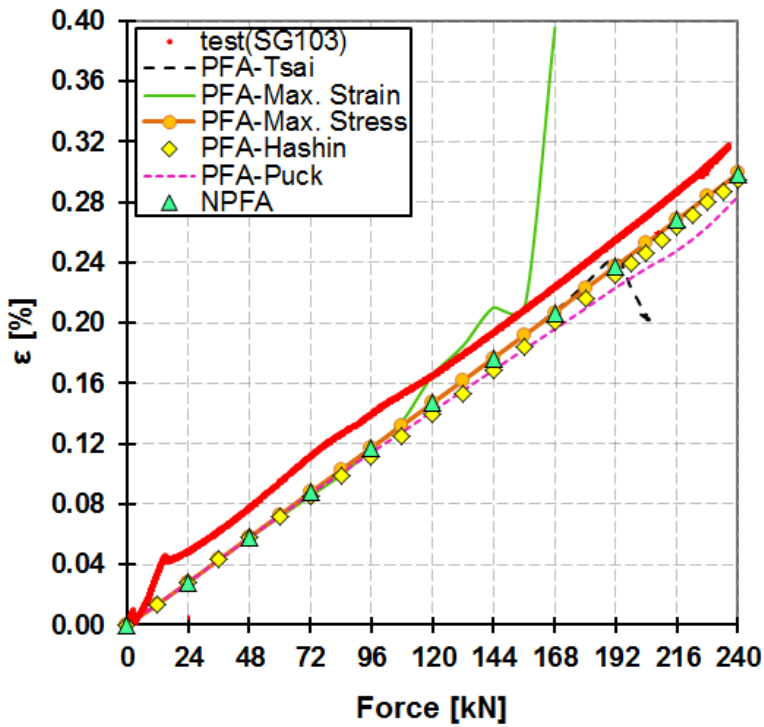
Figure 5.15 Comparison of strain results for SG103 location.

- For the progressive failure analysis with the maximum strain criterion, the deviation from other results initiate before the case for PFA-Tsai. After about 100 kN, an increase in strain occurs. The strain behavior monitored for the

64

PFA-MaxStrain case is unstable after 144 kN; the strain is climbed to extraordinarily high values. The redistribution of forces after failures and degradations in the structure induces such kind of instabilities. Hence, this behavior is meaningless in examining the stiffness of the structure; the data is not comparable with the other results after 144 kN.

- PFA-Hashin and PFA-Puck criteria show no extreme values and almost follow the NPFA. However, actually it is obtained from Figure 5.14 that failure initiates in the structure also for these criteria. Hence, it can be concluded that every failure within the structure does not necessarily affect the strain value that is read at a local area.

The comparison of results for strain gage 105 location can be made by examining the Figure 5.16. Note that in the explanations below, a decrease in strain reading means getting closer to "0" as this strain gage is in compression.

- The estimated strain values by the analysis NPFA are very close to the strain values collected in the test. That is the most compatible model for this comparison. PFA-MxStress also gives very good estimations. All the other analyses yield very unstable strain-force curves.

- The strain vs. force curves of PFA-Hashin and PFA-Puck show very slight oscillations, but may be assumed as almost linear until 144 kN. After that, as compatible with the result presented in Figure 5.1, strain increases until about 180 kN. However, for higher loads, reasonable interpretations cannot be produced since the results only show local instabilities.

- PFA-Tsai shows an almost linear behavior until 168 kN, and a steep decrease started afterwards. As mentioned previously, such kind of actions does not demonstrate any information on the global stiffness of the structure.

- The largest variations in strain vs. force graph are displayed by PFA-MaxStrain. That means, the local unstable behavior due to degradations of the properties and stress redistribution is started almost from the beginning of the analyses.
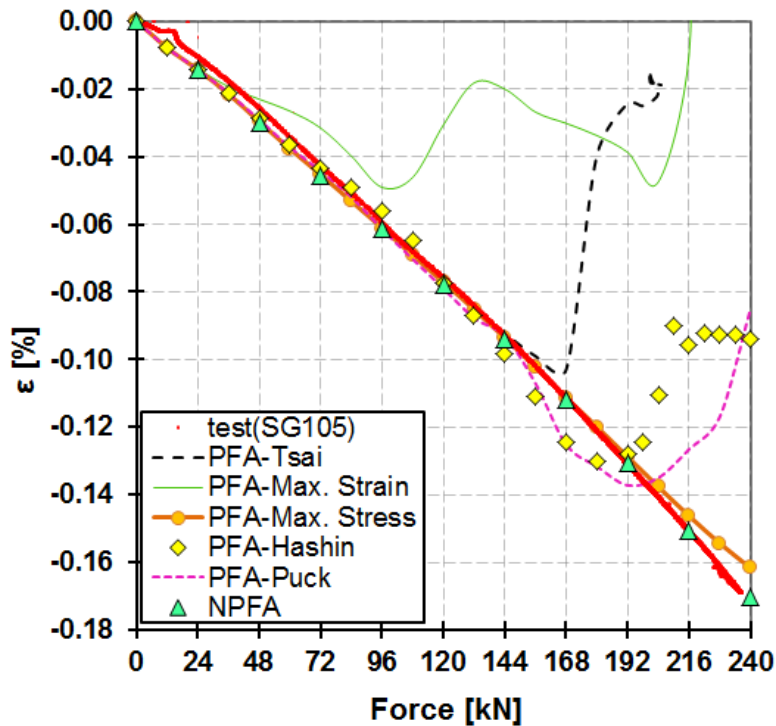
Figure 5.16 Comparison of strain results for SG105 location.

To conclude, the previous figures show that when progressive failure analysis is not applied, strain values can be estimated with high accuracy; whereas in a progressive failure analysis, after degradation is made there may be unexpected increases and decreases in strain values. No interpretations can be done on the global stiffness of the structure from this kind of strain values. However, it can be deduced that property degradation followed by redistribution of the forces causes instabilities in strain values.

In this sense, the importance of reliability of the material properties again proved. The stiffness and hence the strains of the structure is dependent on the calculated failure indices for a progressive failure analysis. Thus, both the reliability of the estimated stresses and allowables utilized has a big role in the assessed strains in the end. When failure is obtained in lower loads than the real case, the stiffness reduction produces unwanted nonlinearities in the system.

The predictions of the various failure criteria and the analysis methods can also be appraised by examining the damage or failure index contours. In the test, no visible damage is occurred in the laminate. There may be failed layers within the composite structure; however, the only layer that can be investigated with naked eye is the top layer and this layer seems to be intact in the areas of interest at 240 kN of tensile loading. Hence, the failure criterion demonstrating the smallest damaged area or failure indices smaller than 1, gives the best prediction. In this section, only damage contours are displayed, since these plots are actually drawn based on the failure index estimations and combining all the effects evaluated by a failure criterion. Interpreting the cumulative effect obtained is easier to understand examining these plots. Failure index plots could be helpful in finding out the

mode of failure that is the most critical for the structure. However, it is enough to evaluate the total influence for this comparison.

Figure 5.17 presents the damage contours of the investigated failure criteria. The plots for the progressive failure analysis outcomes of the maximum stress, the Puck and the Hashin failure criteria are displayed at 240 kN loading. However, as emphasized before, the analyses with the Tsai-Wu and the maximum strain failure criteria cannot reach that force level and the results of these are given for the last load step that can be solved.

Comparing the damage plots presented in Figure 5.17, the largest damage area is obtained for the progressive failure analysis of the maximum strain criterion at a load lower than the other criteria make estimations. The smallest damage area occurs for the maximum stress criterion; and actually, the properties of none of the elements are reduced totally. A maximum reduction of 59% percent is seen for the elements that are near hole and under compression.

For the Tsai-Wu failure criterion, the elements around both holes are completely damaged and the analysis cannot continue after a loading of 205 kN. In this regard, it can be concluded that the Tsai-Wu criterion yields the most critical case, reaching the limit that the analysis can continue at the lowest load. The Hashin failure criterion yields a parallel result nearby the holes as the Tsai-Wu failure criterion; no intact elements are present around the hole at 240 kN and the failure is spreading in 45 degree direction. The Puck failure criterion exhibits a similar damage path as the prediction with the Hashin failure criterion. However, the plots of the Hashin failure criteria show a little more critical situation than the Puck's.

Comparing the results of Figure 5.15 with Figure 5.17, it should be noted that the first criterion giving failure does not have to be the most critical one at the end. For instance, for the Tsai-Wu criterion the first ply failure load is the second highest, whereas it comes out to be the most conservative criterion among all in the end.

Reviewing all the facts mentioned progressive failure with the maximum stress criterion gives the closest prediction for the damage accumulation of the structure. The results from the other criteria over-predicted the damage for this layer. Especially for the maximum strain criterion, the layer seems to be completely deteriorated. This may again be a consequence of unreliable material data; owing to unavailable material strain allowables, results from the stress-based criteria exhibits more rational results than strain-based criterion.
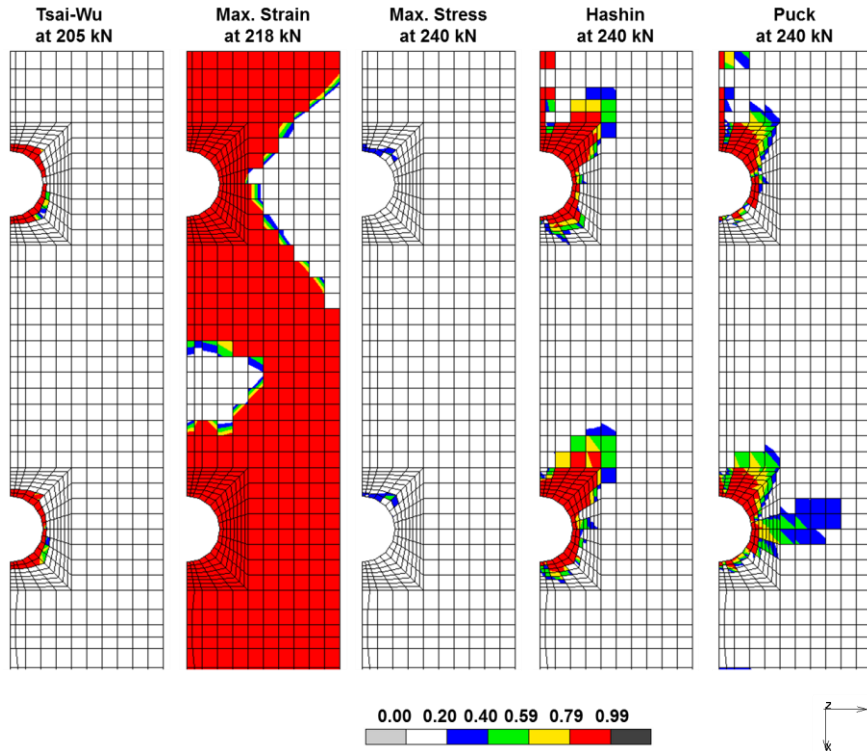
Figure 5.17 Damage plots for layer 65 (carbon fabric 45º) at the indicated loads on figure.

5.4. Modeling Effects on Results

5.4.1. Effect of Number of Through the Thickness Elements

The consequence of changing the number of elements in thickness direction (z-direction of the models) is assessed utilizing the quarter model simulating the tension test.

The comparison is done between two models:

- The first model (named as *quart_6*) has 6 elements in thickness direction. This is exactly the same model as the NPFA presented in the previous sections. The logic behind constructing this model is grouping the plies showing similar lay-ups or materials, i.e. one element for 4 plies of [45/-45]$_s$ carbon lay-up, one element for next 16 plies of [0/45]$_s$, etc. The geometrical dimension of the elements in z-direction is given as equal to the sum of the thicknesses of the plies they comprise.

- Second model (named as *quart_65*) formed by 65 elements through the thickness; one element for each ply. The dimension of the element in z-direction is specified like in the case of first model; hence the height of the element is the ply thickness.
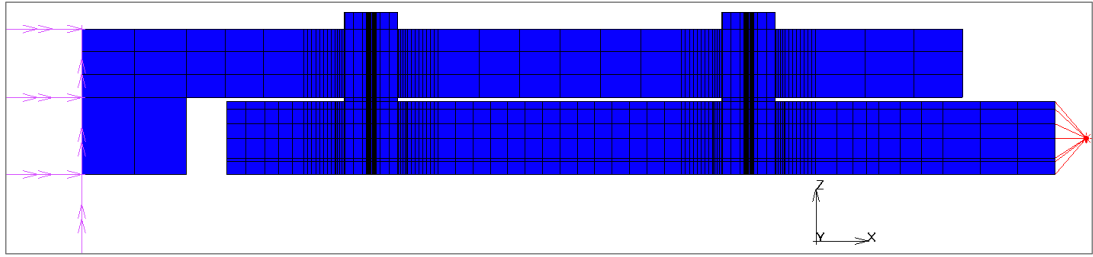
Figure 5.18 First model: "quart_6".
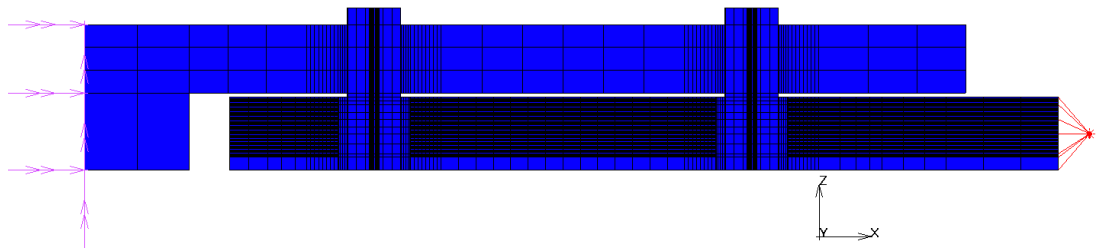
Figure 5.19 Second model: "quart_65".

In both models:

- Contact is defined between all the contacting bodies but the interference fit of bushing with the lug is not taken into account

- Tensile load is applied at a point which is not a part of analyzed structure and transferred to the laminate with a RBE2 element which defines a rigid link that the load transmits through the load application point to the end nodes of the composite laminate.

The strains on top of laminate obtained from the analyses and test are compared and the results are depicted in Figures 5.20 and 5.21. As can be seen in figures, utilizing 65 elements in thickness direction does not contribute to the accuracy of the result much in terms of strain comparison at the strain gage 103 and strain gage 105 locations. However, utilizing six elements in thickness direction is far more advantageous in analysis time compared to using 65 elements. Having convinced using more elements in thickness direction does not enhance the result regarding the strain values, the analyses conducted in this thesis study are performed using six elements in thickness direction.
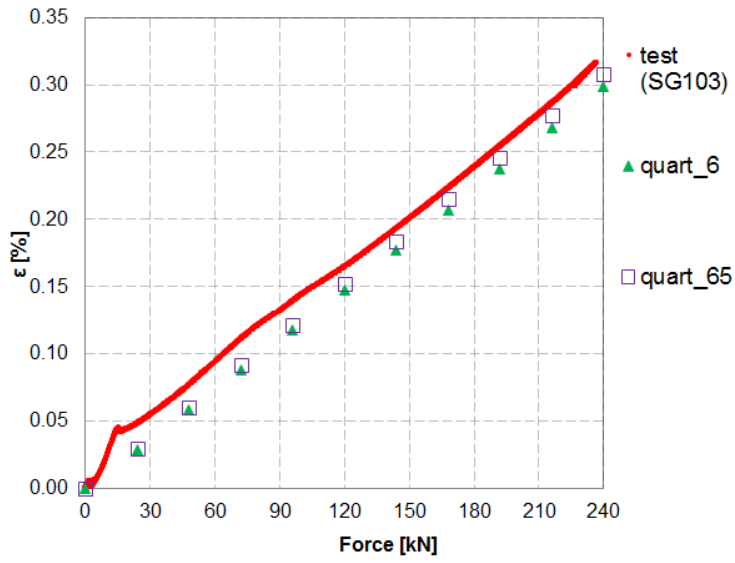
Figure 5.20 Comparison of strain results of quart_6 and quart_65 models and test results for SG103 location.
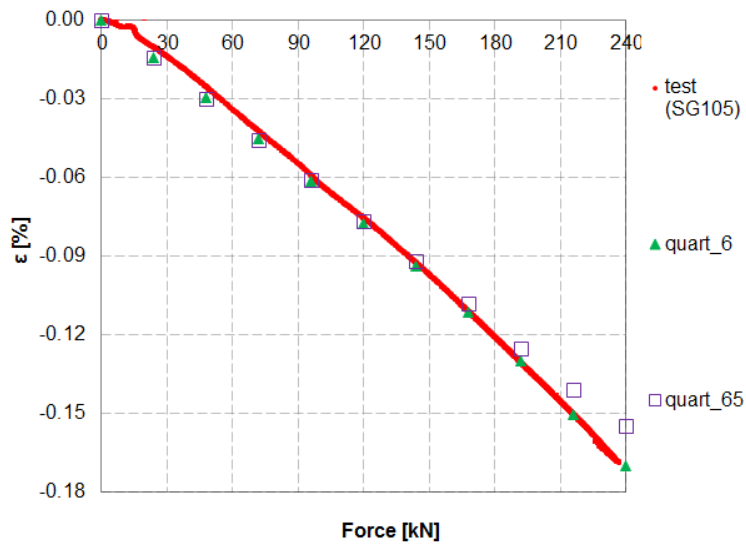
Figure 5.21 Comparison of strain results of quart_6 and quart_65 models and test results for SG105 location.

CHAPTER 6

CONCLUSION and FUTURE WORK

In this study, finite element analyses and testing of a thick composite structure are performed. The purpose is to suggest a reliable analysis method to predict the failure of the thick laminate that has a hybrid structure and contains holes. The analysis procedures are aimed to be verified by a tension test.

The investigated laminated composite structure is constituted from carbon fabric, unidirectional glass and foam material. There are bushings installed to the holes of the laminate with interference fit. Bolts are used in attaching this assembly to a steel grip. A three dimensional-quarter finite element model is constructed to investigate this assembly. The connections between all the parts are defined introducing a contact algorithm. A tension load is applied to the laminated composite and the load is transmitted throughout the assembly in accordance with the contact descriptions.

Finite element analyses with and without progressive failure are conducted applying various failure criteria. The advantages and disadvantages of analysis with progressive failure are discussed.

Tension test of this analyzed structure was carried out in order to verify the analyses methods. From the top and bottom of the specimen surface strain data is collected during the test.

The compatibility of the outcomes of the analyses with the test is evaluated by making comparison with the strain data collected in the test. Additionally, the assessment of the failure predictions of the analyses with each other and the consistency of these results with the result of the tension test are made. This is achieved by investigating the images that the analyses produce for failure visualization with the result of the visual inspection of the specimen after the test.

The influence of modeling with different number of elements is also studied and the method of comparison with strain data is again used for evaluation.

According to the results obtained in this study, the following conclusions are made:

- Exhibiting almost no property diminution and displaying no serious damage progression until the loading investigated in the test, also representing nearly an intact structure for the analysis without progressive failure analysis, the maximum stress criterion is obtained to give the most compatible results with tests.

- The Tsai-Wu and the maximum strain failure represent the most critical cases in failure prediction. Although, the maximum strain criterion plots show larger areas of failure (or damage), the Tsai-Wu criterion yields the most critical case. The complete failure of PFA-Tsai occurs at a lower load than all the other criteria. Moreover, it suddenly happens as long as the elements around holes are failed; whereas, the maximum strain criterion allows spread of the failure extensively within the structure. If damage

progression were a sign of damage tolerance, it would have been concluded that estimation with the maximum strain criterion shows the structure as having a high damage tolerance, while for computation with the Tsai-Wu failure criterion, damage tolerance of the structure seems to be very low.

- Comparison of the strain results obtained from the finite element analyses and the test reveal that the model can make successful estimations of strains. Strain results of some of the analyses deviate from the strain values of the test as a consequence of the instabilities induced by the redistribution of forces due to progressive failure. If such a behavior is identified in the results, no interpretations about the stiffness of the structure can be made after this point. However, these local effects do not change the conclusion that the model constructed gives compatible results with the test.

- Even though, acceptable predictions are accomplished by the analyses with the maximum stress criterion, the reason of not having very well suited failure predictions with the other criteria is an accumulated result of various reasons: not having reliable material allowables, the over-conservative characteristics of the failure criteria, assumptions made in modeling. The over-conservative characteristics of the criteria are also reviewed broadly in literature. A dramatic evaluation on the final failure strength of the criteria reveals that the accuracy of the criteria is in the range of ±50% accuracy [34]. Furthermore, it is found that the methods introduced so far for final failure prediction cannot achieve very accurate solutions when the laminate is multidirectional, like the one investigated in this study. The accuracy of the method is very sensitive to changes that when the applied load changes, a complete modification of method would be required. Another clarification is introduced by Hashin, himself. He claims that the method he presented is only valid for failure prediction of unidirectional lamina. Hence, estimation of failure of laminates, which shows complicated failure behaviors until collapse, may not give very promising results. He defends failure prediction of a laminate necessitates analysis of damage and still, after all the advances in literature, the capability is not adequate [36].

- Comparison of the analyses results with the test proved that also for this structure application of first ply failure approach is too conservative for design purposes. If this method is to be used, a careful evaluation of which failure will be important and which will be neglected to get rid of unnecessarily conservative designs. This method cannot give any information on the consequences of a failure. However, progressive failure analysis evaluates the effect of initiation of a failure and provides a more reliable basis than the assessment of the designer.

- Some problems are identified in the execution of the test. For instance, the failure of the bolt on the load introduction side was not the end that is intended. Moreover, the stroke readings of the machine are not suitable for comparison with the analysis results.

In the outlook of these conclusions, the following are suggested for future studies:

- Before conducting a failure analysis, it is important to be more confident on the material properties used. Reviewing all the results attained, the importance of utilizing reliable material properties is understood. With the assumed values of the properties, no definite judgement on the prediction capabilities of the failure criteria can be reached. For instance, when the

maximum strain criterion gives the largest failed area, the only comment can be made was that if reliable strain allowables were available, this criterion would be specified as giving the most conservative results among all. In this case, it is not certain if this behavior is a consequence of the criteria used or the properties that are assumed. This study is a part of an ongoing project, thus in the later stages of the project a great effort should be spent to create a reliable material database, especially to obtain strain allowables and the properties in thickness direction which are the basic causes of uncertainties in the comments of this model.

- As a result of the survey on progressive failure analysis it was concluded that besides the advantages of progressive failure analysis, the analyst shall be very careful implementing this method as the reliability of the method is very sensitive to changes in modeling parameters. One of the most important of these parameters is the element size, that dependency is also proved by some studies [23, 57, 58]. In addition, it is trivial that the calculated initial and ultimate failure loads by progressive failure analysis are dependent on the procedure of failure prediction and degradation. Additionally, for the thick structure the number of elements used in thickness direction can be important. This evaluation initiated but the effects cannot be investigated in detail. Furthermore, numerical convergence check methods have also great influence on the results. The effect of contact modeling is another thing that can be investigated in scope of this study. Actually the evaluation started, however reasonable convergence cannot be obtained and the results are not presented within this thesis report. For instance, the outcomes like, the jumps in strain values due to redistribution of forces after degradation may be enhanced by following the suggestions presented.

- The test specimen shall be modified to give failure in the intended area. The ultimate failure of the composite cannot be determined because of the failure of the bolts before the failure of the specimen. Hence, no comparison on the final failure strength of the specimen can be done.

REFERENCES

[1] Mazumdar SK. Composites Manufacturing: Materials, Product, and Process Engineering: CRC Press, 2001.

[2] Zimmermann K, Zenkert D, Siemetzki M. Testing and analysis of ultra thick composites. Composites Part B: Engineering. 2010;41:326-36.

[3] P. MAIMI JAM, P.P. CAMANHO. A Three-Dimensional Damage Model for Transversely Isotropic Composite Laminates. Journal of Composite Materials: Journal of Composite Materials; 2008.

[4] McCarthy CT, McCarthy MA, Lawlor VP. Progressive damage analysis of multi-bolt composite joints with variable bolt–hole clearances. Composites Part B: Engineering. 2005;36:290-305.

[5] Jones RM. Mechanics of Composite Materials. 2nd ed: Taylor&Francis Inc., 1999.

[6] SPENCER AJM. Continuum Theory of The Mechanics of Fibre-Reinforced Composites: Springer, 1984.

[7] Reddy JN. Mechanics of laminated composite plates and shells: Theory and analysis. 2nd ed: CRC press, 2004.

[8] Knight NF, Jr. Factors Influencing Progressive Failure Analysis Predictions for Laminated Composite Structure. 49th AIAA/ASME/ASCE/AHS/ASC Structures, Structural Dynamics and Materials Conference; 7-10 Apr. 2008; Schaumburg, IL; United States: NASA; 2008.

[9] Czichon S, Zimmermann K, Middendorf P, Vogler M, Rolfes R. Three-dimensional stress and progressive failure analysis of ultra thick laminates and experimental validation. Composite Structures. 2011;93:1394-403.

[10] Shepheard B, Jackson D, Dixon M, Sims G. Testing of thick carbon fibre laminate composites:comparison of thick with thin coupons, current standards and product case study. 36th International Sampe Techical Conference. San Diego, CA2004. p. 11.

[11] Gower MRL, Shaw RM. Development of test methods for measuring thick section tensile and compression properties of polymer matrix composites Middlesex: National Physics Laboratory; 2011.

[12] Lagace P, Brewer J, Kassapoglou C. The effect of thickness on interlaminar stresses and delamination in straigth-edged laminates. Journal of Composites and Technology. 1987;9:81-7.

[13] Jackson KE, Kellas S, Morton J. Scale effects in the response and failure of fiber reinforced composite laminates loaded in tension and in flexure. Journal of Composite Materials. 1992;26:2674-705.

[14] Shepheard B, Jackson D, Dixon M, Sims G. Predicting the performance and failure of thick complex carbon fibre laminates. http://www.deepsea-eng.com/media/technical-papers/Predicting-the-Performance-and-Failure-of-Thick-Complex-Carbon-Fibre-Laminates.: Deepsea; 2005.

[15] Park H-J. Bearing failure analysis of mechanically fastened joints in composite laminates. Composite Structures. 2001;53:199-211.

[16] Wong CMS, Matthews FL. A Finite element analysis of single and two-hole bolted joints in fibre reinforced plastic. Journal of Composite Materials. 1981;15:481-90.

[17] Chang FK, Scott RA, Springer GS. Failure of composite laminates containing pin loaded holes - method of solution. Journal of Composite Materials. 1982;16:470-94.

[18] Chutima S, Blackie AP. Effect of pitch distance, row spacing, end distance and bolt diameter on multi-fastened composite joints. Composites Part A: Applied Science and Manufacturing. 1996;27:105-10.

[19] Madenci E, Shkarayev S, Sergeev B, Oplinger DW, Shyprykevich P. Analysis of composite laminates with multiple fasteners. International Journal of Solids and Structures. 1998;35:1793-811.

[20] Ireman T. Design of Composite Structures Containing Bolt Holes and Open Holes. Stockholm, Sweden: Kungliga Tekniska Hönskolan, 1999.

[21] McCarthy M. BOJCAS: Bolted Joints in Composite Aircraft Structures. Air and Space Europe. 2001;3:139-42.

[22] Park H-J. Effects of stacking sequence and clamping force on the bearing strengths of mechanically fastened joints in composite laminates. Composite Structures. 2001;53:213-21.

[23] Satyanarayana A, Przekop A. Predicting failure progression and failure loads in composite open-hole tension coupons. Hampton, VA: NASA Langley Research Center; 2010.

[24] Puck A, Schürmann H. Failure analysis of FRP laminates by means of physically based phenomenological models. Composites Science and Technology. 2002;62:1633-62.

[25] Puck A, Schürmann H. Failure Analysis Of FRP Laminates By Means Of Physically Based Phenomenological Models. Composites Science and Technology. 1998;58:1045-67.

[26] Bogetti TA, Hoppel CPR, Harik VM, Newill JF, Burns BP. Predicting the nonlinear response and progressive failure of composite laminates. Composites Science and Technology. 2004;64:329-42.

[27] Chou PC, Carleone J, Hsu CM. Elastic Constants of Layered Media. Journal of Composite Materials. 1972;6:80-93.

[28] Bogetti TA, Hoppel CP, Drysdale WH. Three-Dimensional Effective Property and Strength Prediction of Thick Laminated Composite Media. U.S. Army Research Laboratory Weapons Technology Directorate; 1995.

[29] Pineda EJ, Waas AM, Bednarcyk BA, Collier CS, Yarrington PW. A Novel Multiscale Physics Based Progressive Failure Methodology for Laminated Composite Structures. NASA Glenn Research Center; 2008.

[30] Cuntze RG. The predictive capability of failure mode concept-based strength criteria for multi-directional laminates—part B. Composites Science and Technology. 2004;64:487-516.

[31] Satyanarayana A, Bogert PB, Chunchu PB. The Effect of Delamination on Damage Path and Failure Load Prediction for Notched Composite Laminates. 48th AIAA/ASME/ASCE/AHS/ASC Structures, Structural Dynamics, and Materials Conference; 23-26 Apr 2007. Waikiki, HI; United States2007.

[32] Bogert PB, Satyanarayana A, Chunchu PB. Comparison of Damage Path Predictions for Composite Laminates by Explicit and Standard Finite Element Analysis Tools. 47th AIAA/ASME/ASCE/AHS/ASC Structures, Structural Dynamics, and Materials Conference; 1-4 May 2006 Newport, RI; United States2006.

[33] Green BG, Wisnom MR, Hallett SR. An experimental investigation into the tensile strength scaling of notched composites. Composites Part A: Applied Science and Manufacturing. 2007;38:867-78.

[34] Hinton MJ, Kaddour AS, Soden PD. A comparison of the predictive capabilities of current failure theories for composite laminates, judged against experimental evidence. Composites Science and Technology. 2002;62:1725-97.

[35] Kaddour AS, Hinton MJ, Soden PD. A comparison of the predictive capabilities of current failure theories for composite laminates: Additional contributions. Composites Science and Technology. 2004;64:449-76.

[36] Hinton MJ, Kaddour AS, Soden PD. Chapter 1.1 - The world-wide failure exercise: Its origin, concept and content. In: Hinton MJ, Kaddour AS, P.D. SodenA2 - M.J. Hinton ASK, Soden PD, editors. Failure Criteria in Fibre-Reinforced-Polymer Composites. Oxford: Elsevier; 2004. p. 2-28.

[37] Soden PD, Kaddour AS, Hinton MJ. Recommendations for designers and researchers resulting from the world-wide failure exercise. Composites Science and Technology. 2004;64:589-604.

[38] Pinho ST, Davila CG, Camanho PP, Iannucci L, Robinson P. Failure Models and Criteria for FRP Under In-Plane or Three-Dimensional Stress States Including Shear Non-Linearity. Hampton, VA: NASA Langley Research Center; 2005.

[39] Hinton MJ, Kaddour AS, Soden PD. A further assessment of the predictive capabilities of current failure theories for composite laminates: comparison with experimental evidence. Composites Science and Technology. 2004;64:549-88.

[40] Gotsis PK, Chamis CC, Minnetyan L. Prediction of composite laminate fracture: micromechanics and progressive fracture. Composites Science and Technology. 1998;58:1137-49.

[41] Mayes JS, Hansen AC. Composite laminate failure analysis using multicontinuum theory. Composites Science and Technology. 2004;64:379-94.

[42] Huang Z-M. A bridging model prediction of the ultimate strength of composite laminates subjected to biaxial loads. Composites Science and Technology. 2004;64:395-448.

[43] Zinoviev PA, Grigoriev SV, Lebedeva OV, Tairova LP. The strength of multilayered composites under a plane-stress state. Composites Science and Technology. 1998;58:1209-23.

[44] Cuntze RG, Freund A. The predictive capability of failure mode concept-based strength criteria for multidirectional laminates. Composites Science and Technology. 2004;64:343-77.

[45] Liu K-S, Tsai SW. A progressive quadratic failure criterion for a laminate. Composites Science and Technology. 1998;58:1023-32.

[46] Kuraishi A, Tsai SW, Liu KKS. A progressive quadratic failure criterion, part B. Composites Science and Technology. 2002;62:1683-95.

[47] Achieving Composite Progressive Failure with Multiscale Analysis. Firehole Composites.

[48] Bogetti TA, Hoppel CPR, Harik VM, Newill JF, Burns BP. Predicting the nonlinear response and failure of composite laminates: correlation with experimental results. Composites Science and Technology. 2004;64:477-85.

[49] MSC.Software. Marc 2010 User Documentation Volume A: Theory and User Information. U.S.A: MSC.Software Corporation, 2010.

[50] Ochoa OO, Reddy JN. Finite Element Analysis of Composite Laminates: Kluwer Academic Publishers, 1992.

[51] Department of Defence USoA. Metallic materials and elements for aerospace vehicle structures. 2003.

[52] MSC.Software. MSC.Marc Nonlinear analysis for engineering applications and manufacturing process. http://www.mscsoftware.com/assets/MA2005JULZZZLTDAT.pdf.

[53] MSC.Software. Marc 2010 User Documentation Volume B: Element Library. U.S.A: MSC.Software Corporation, 2010.

[54] Kuhlmann G, Rolfes R. A hierarchic 3D finite element for laminated composites. International Journal for Numerical Methods in Engineering. 2004;61:96-116.

[55] Teknik Destek Grubu: Aİ8b Kullanma Kılavuzu. Ankara2007.

[56] Composite Damage in Progressive Failure Analysis. http://simcompanion.mscsoftware.com.2011.

[57] Camanho PP, Maimí P, Dávila CG. Prediction of size effects in notched laminates using continuum damage mechanics. Composites Science and Technology. 2007;67:2715-27.

[58] Lapczyk I, Hurtado JA. Progressive damage modeling in fiber-reinforced materials. Composites Part A: Applied Science and Manufacturing. 2007;38:2333-41.